

Supplementary Information

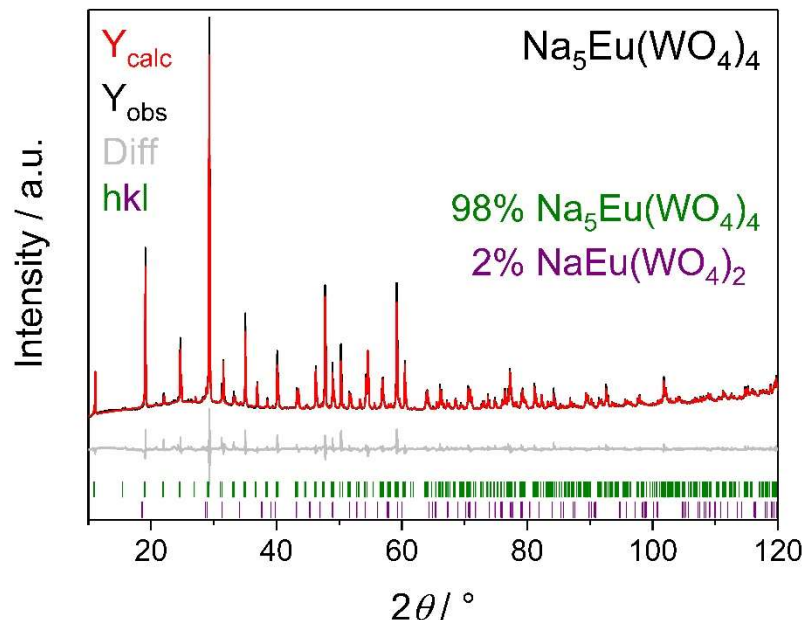


Fig. S1: Rietveld-Refinement of $\text{Na}_5\text{Eu}(\text{WO}_4)_4$ prepared by flux synthesis; further details can be found in Table S3.

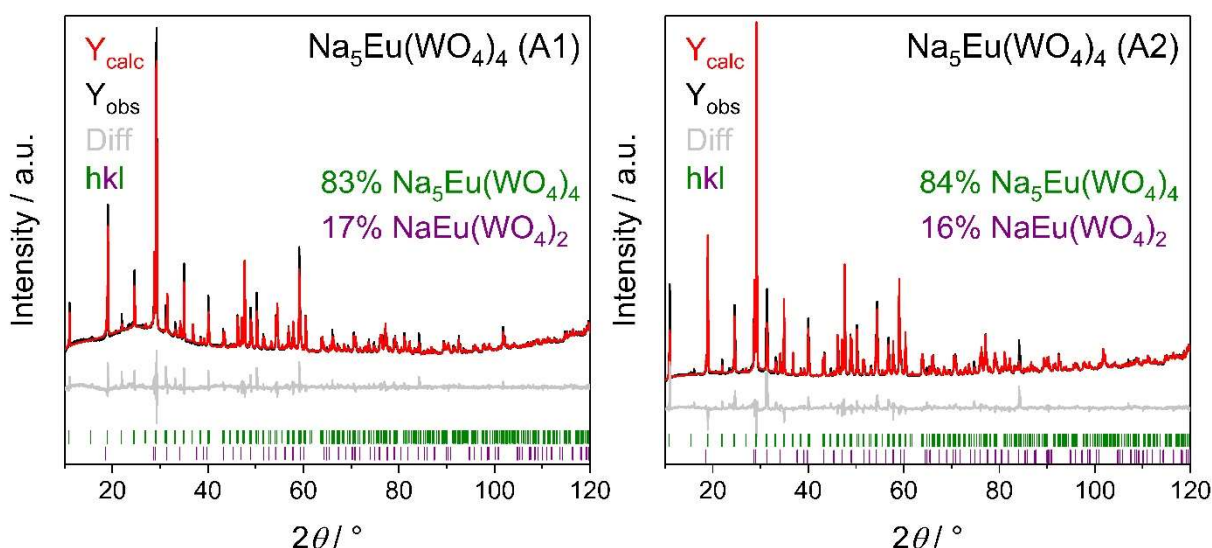


Fig. S2: Rietveld refinements of $\text{Na}_5\text{Eu}(\text{WO}_4)_4$ prepared by standard solid state reaction at 600°C (A1) (left) and 700°C (A2) (right); the refinements yielded in R_{wp} of 2.24% and 4.23%, R_{Bragg} of 1.29% and 2.91% for $\text{Na}_5\text{Eu}(\text{WO}_4)_4$ and 0.72% and 1.77% for $\text{NaEu}(\text{WO}_4)_2$, respectively.

Table S1. Crystal data and structure refinements of $\text{NaEu}(\text{WO}_4)_2$ and $\text{Na}_5\text{M}(\text{WO}_4)_4$ ($\text{M} = \text{Ce}, \text{Pr}, \text{Nd}, \text{Sm}, \text{Eu}$) determined from single-crystal data^a

	$\text{NaEu}(\text{WO}_4)_2$	$\text{Na}_5\text{Ce}(\text{WO}_4)_4$	$\text{Na}_5\text{Pr}(\text{WO}_4)_4$	$\text{Na}_5\text{Nd}(\text{WO}_4)_4$	$\text{Na}_5\text{Sm}(\text{WO}_4)_4$	$\text{Na}_5\text{Eu}(\text{WO}_4)_4$
CSD-No.	1986866	1986870	1986859	1986871	1986862	1986865
$M / \text{g mol}^{-1}$	670.65	1246.47	1247.26	1250.59	1256.70	1258.31
Crystal size / mm^3	$0.04 \times 0.04 \times 0.03$	$0.07 \times 0.03 \times 0.03$	$0.04 \times 0.04 \times 0.04$	$0.04 \times 0.04 \times 0.03$	$0.04 \times 0.04 \times 0.02$	$0.10 \times 0.06 \times 0.03$
Temperature / K				300(3)		
Space group				$I4_1/a$ (No. 88)		
a / pm	526.24(1)	1158.57(3)	1157.65(2)	1155.89(4)	1151.61(4)	1149.98(4)
c / pm	1140.78(3)	1152.47(4)	1147.97(2)	1147.22(4)	1142.31(4)	1140.61(4)
Volume / 10^6 pm^3	316.07(3)	1546.94(10)	1538.46(6)	1532.78(12)	1514.94(12)	1508.40(12)
Z	2			4		
$\rho_{\text{calcd}} / \text{g cm}^{-3}$	7.05	5.35	5.39	5.42	5.51	5.54
Absorption coefficient μ / mm^{-1}	46.2	32.7	33.1	33.5	34.3	34.7
$F(000) / e$	572	2148	2152	2156	2164	2168
Radiation; wavelength $\lambda / \text{\AA}$				MoK α ; 0.71073		
Diffractometer				Bruker D8 Venture		
Absorption correction				Multi-scan		
Transmission (min; max)	0.6338; 0.7503	0.6678; 0.7478	0.6011; 0.7488	0.5281; 0.7472	0.5921; 0.7479	0.6001; 0.7483
Index range $h k l$	-9/9 -9/9 -21/21	-14/16 -15/16 -15/15	-19/21 -21/21 -20/20	-17/16 -16/17 -17/17	-18/19 -19/19 -19/19	-20/20 -15/20 -20/20
θ range / deg	4.265–41.863	2.493–29.415	2.499–40.487	2.501–33.497	2.511–36.979	2.515–39.996
Reflections collected	21433	9235	26586	13470	18168	16901
Independent reflections	546	1062	2455	1504	1937	2337
R_{int}	0.0284	0.0325	0.0504	0.056	0.0403	0.0406
Obs. reflections ($I > 2 \sigma(I)$)	472	1008	2191	1277	1722	2025
Refined parameters	16	59	60	60	60	60
R_1 (all data)	0.018	0.0321	0.024	0.0322	0.023	0.0258
wR ₂ (all data)	0.034	0.0719	0.0298	0.0362	0.0321	0.0356
GooF	1.12	1.342	1.076	1.038	1.038	1.026
Residual electron density (max; min) / $e^- \text{\AA}^{-3}$	2.08; -1.51	2.16; -2.13	1.16; -1.22	1.08; -1.18	1.56; -1.10	1.41; -1.18

^a The respective standard deviations are given in parentheses.

Table S2. Crystal data and structure refinements of $\text{Na}_5\text{M}(\text{WO}_4)_4$ ($\text{M} = \text{Gd}, \text{Tb}, \text{Ho}, \text{Tm}, \text{Yb}, \text{Bi}$) determined from single-crystal data^a

	$\text{Na}_5\text{Gd}(\text{WO}_4)_4$	$\text{Na}_5\text{Tb}(\text{WO}_4)_4$	$\text{Na}_5\text{Ho}(\text{WO}_4)_4$	$\text{Na}_5\text{Tm}(\text{WO}_4)_4$	$\text{Na}_5\text{Yb}(\text{WO}_4)_4$	$\text{Na}_5\text{Bi}(\text{WO}_4)_4$
CSD-No.	1986868	1986861	1986869	1986863	1986867	1986858
$M / \text{g mol}^{-1}$	1263.60	1265.27	1271.28	1275.28	1279.39	1315.33
Crystal size / mm^3	$0.06 \times 0.04 \times 0.04$	$0.08 \times 0.04 \times 0.03$	$0.06 \times 0.06 \times 0.04$	$0.08 \times 0.05 \times 0.04$	$0.05 \times 0.05 \times 0.04$	$0.08 \times 0.04 \times 0.03$
Temperature / K			300(3)			
Space group			$I4_1/a$ (No. 88)			
a / pm	1147.96(4)	1146.90(5)	1143.99(4)	1139.99(6)	1139.65(10)	1154.33(4)
c / pm	1137.79(4)	1137.91(6)	1134.69(5)	1129.85(6)	1129.32(11)	1141.36(4)
Volume / 10^6 pm^3	1499.39(12)	1496.78(15)	1484.98(12)	1468.33(17)	1466.8(3)	1520.84(12)
Z			4			
$\rho_{\text{calcd}} / \text{g cm}^{-3}$	5.60	5.61	5.69	5.77	5.79	5.75
Absorption coefficient μ / mm^{-1}	35.2	35.5	36.4	37.4	37.8	41.9
$F(000) / e$	2172	2176	2184	2192	2196	2248
Radiation; wavelength $\lambda / \text{\AA}$			MoK α ; 0.71073			
Diffractometer			Bruker D8 Venture			
Absorption correction			Multi-scan			
Transmission (min; max)	0.5701; 0.7492	0.5804; 0.7479	0.4945; 0.7489	0.5591; 0.7506	0.4954; 0.7477	0.6549; 0.7459
Index range $h k l$	-20/16 -20/20 -	-19/19 -19/14 -19/19	-19/19 -19/13 -19/19	-20/20 -20/18 -20/20	-12/19 -18/19 -18/18	-15/15 -15/15 -15/15
θ range / deg	2.520–40.496	2.521–37.475	2.528–37.999	2.538–39.496	2.539–36.400	2.510–29.246
Reflections collected	23034	15674	15782	18502	13271	12840
Independent reflections	2397	1961	2021	2215	1795	1040
R_{int}	0.0459	0.044	0.0378	0.0449	0.0468	0.0521
Obs. reflections ($I > 2 \sigma(I)$)	2116	1718	1795	1940	1533	912
Refined parameters	60	60	60	60	60	60
R_1 (all data)	0.0243	0.0282	0.0252	0.0266	0.03	0.025
wR ₂ (all data)	0.0349	0.04	0.0354	0.0363	0.0391	0.0307
GooF	1.081	1.095	1.086	1.076	1.049	1.069
Residual electron density (max; min) / $e^- \text{\AA}^{-3}$	2.05; -1.12	1.99; -1.21	1.45; -1.19	1.43; -1.30	1.28; -1.50	1.11; -0.84

^a The respective standard deviations are given in parentheses.

Table S3. Crystal data and structure refinements of $\text{Na}_5\text{M}(\text{WO}_4)_4$ ($\text{M} = \text{La}, \text{Pr}, \text{Sm}, \text{Eu}, \text{Gd}, \text{Tb}$) determined from powder XRD data via Rietveld refinement^a

	$\text{Na}_5\text{La}(\text{WO}_4)_4$	$\text{Na}_5\text{Pr}(\text{WO}_4)_4$	$\text{Na}_5\text{Sm}(\text{WO}_4)_4$	$\text{Na}_5\text{Eu}(\text{WO}_4)_4$	$\text{Na}_5\text{Gd}(\text{WO}_4)_4$	$\text{Na}_5\text{Tb}(\text{WO}_4)_4$
CSD-No.	1986874					
$M / \text{g mol}^{-1}$	1245.21	1247.21	1256.66	1258.26	1263.55	1265.23
Temperature / K			300(3)			
Space group			$I4_1/a$ (No. 88)			
a / pm	1163.319(11)	1158.140(15)	1152.270(14)	1150.503(12)	1149.044(13)	1147.108(14)
c / pm	1154.299(13)	1148.516(17)	1142.453(16)	1140.722(14)	1139.496(15)	1137.197(16)
Volume / 10^6 pm^3	1562.13(3)	1540.49(5)	1516.86(4)	1509.92(4)	1504.48(4)	1496.39(4)
Z			4			
$R_{\text{Bragg}} / \%$	2.23	1.973	1.527	1.203	1.252	0.951
$\rho_{\text{calcd}} / \text{g cm}^{-3}$	5.30	5.38	5.50	5.54	5.58	5.62
Radiation; wavelength $\lambda / \text{\AA}$			$\text{CuK}\alpha$; 1.54184			
Diffractometer			Seifert 3003 TT			
2θ range / deg			5–120			
No. of independent parameters	49	49	49	49	49	49
R_{wp}	0.0375	0.0366	0.0382	0.0253	0.029	0.02257
Side phase	$\text{NaLa}(\text{WO}_4)_2$	$\text{NaPr}(\text{WO}_4)_2$	$\text{NaSm}(\text{WO}_4)_2$	$\text{NaEu}(\text{WO}_4)_2$	$\text{NaGd}(\text{WO}_4)_2$	$\text{NaTb}(\text{WO}_4)_2$
Fraction of side phase / wt.-% ^b	4.15	2.89	4.32	2.22	1.2	0.9
Space group			$I4_1/a$ (No. 88)			
a / pm	535.799(18)	531.45(3)	527.10(2)	525.72(4)	524.80(8)	523.09(11)
c / pm	1165.51(7)	1154.88(13)	1143.46(10)	1140.84(17)	1137.1(3)	1135.0(5)
Volume / 10^6 pm^3	334.60(3)	326.19(6)	317.70(4)	315.31(7)	313.16(13)	310.58(19)
Z			2			
$R_{\text{Bragg}} / \%$	1.233	1.211	1.135	0.689	1.099	0.895

^a The respective standard deviations are given in parentheses. ^b The $\text{NaM}(\text{WO}_4)_2$ side phase was not refined under a fraction of 1 wt.%.

Table S4. Crystal data and structure refinements of $\text{Na}_5\text{M}(\text{WO}_4)_4$ ($\text{M} = \text{Dy}, \text{Ho}, \text{Er}, \text{Lu}, \text{Y}$) determined from powder XRD data via Rietveld refinement^a

	$\text{Na}_5\text{Dy}(\text{WO}_4)_4$	$\text{Na}_5\text{Ho}(\text{WO}_4)_4$	$\text{Na}_5\text{Er}(\text{WO}_4)_4$	$\text{Na}_5\text{Lu}(\text{WO}_4)_4$	$\text{Na}_5\text{Y}(\text{WO}_4)_4$
CSD-No.			1986873	1986876	1986875
$M / \text{g mol}^{-1}$	1268.80	1271.23	1273.56	1281.27	1195.21
Temperature / K			300(3)		
Space group			$I4_1/a$ (No. 88)		
a / pm	1145.626(15)	1143.999(12)	1142.573(13)	1138.701(12)	1143.616(11)
c / pm	1135.742(17)	1134.018(14)	1132.408(14)	1128.231(13)	1134.047(12)
Volume / 10^6 pm^3	1490.61(4)	1484.13(4)	1478.33(4)	1462.91(3)	1483.17(3)
Z			4		
$R_{\text{Bragg}} / \%$	1.52	1.32	1.6	1.63	1.69
$\rho_{\text{calcd}} / \text{g cm}^{-3}$	5.66	5.69	5.72	5.82	5.35
Radiation; wavelength $\lambda / \text{\AA}$			$\text{CuK}\alpha; 1.54184 \text{\AA}$		
Diffractometer			Seifert 3003 TT		
2θ range / deg			5–120		
No. of independent parameters	46	46	46	49	46
R_{wp}	0.0375	0.0322	0.0394	0.036	0.0371
Side phase	-	-	-	$\text{NaLu}(\text{WO}_4)_2$	-
Fraction of side phase / wt.-% ^b	-	-	-	2.82	-
Space group	-	-	-	$I4_1/a$ (No. 88)	-
a / pm	-	-	-	516.39(3)	-
c / pm	-	-	-	1117.20(11)	-
Volume / 10^6 pm^3	-	-	-	297.91(4)	-
Z	-	-	-	2	-
$R_{\text{Bragg}} / \%$	-	-	-	1.93	-

^a The respective standard deviations are given in parentheses. ^b The $\text{NaM}(\text{WO}_4)_2$ side phase was not refined under a fraction of 1 wt.%.

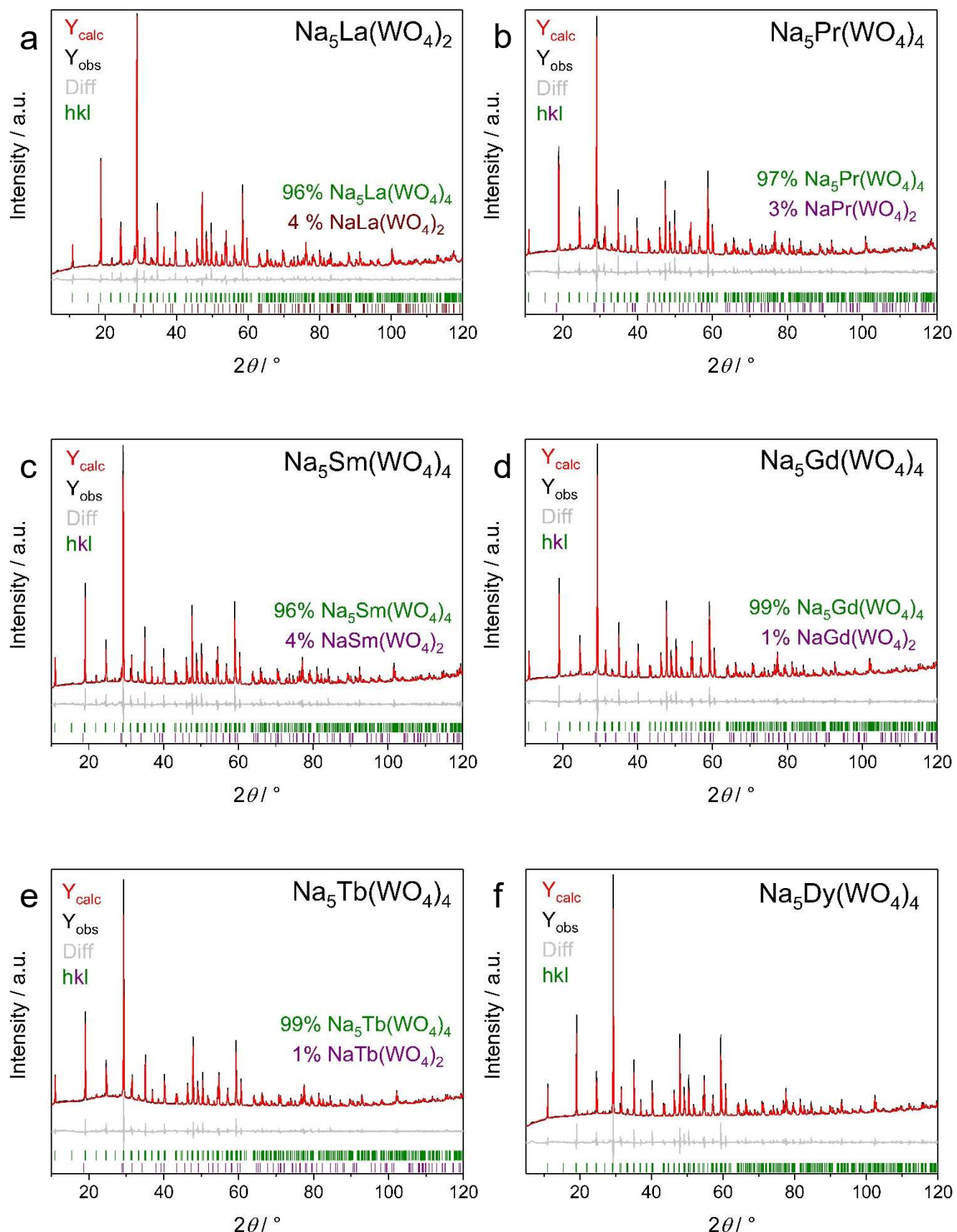


Fig. S3: Rietveld refinements of (a) $\text{Na}_5\text{La}(\text{WO}_4)_4$, (b) $\text{Na}_5\text{Pr}(\text{WO}_4)_4$, (c) $\text{Na}_5\text{Sm}(\text{WO}_4)_4$, (d) $\text{Na}_5\text{Gd}(\text{WO}_4)_4$, (e) $\text{Na}_5\text{Tb}(\text{WO}_4)_4$ and (f) $\text{Na}_5\text{Dy}(\text{WO}_4)_4$ prepared by flux synthesis; further details can be found in Tables S3 and S4.

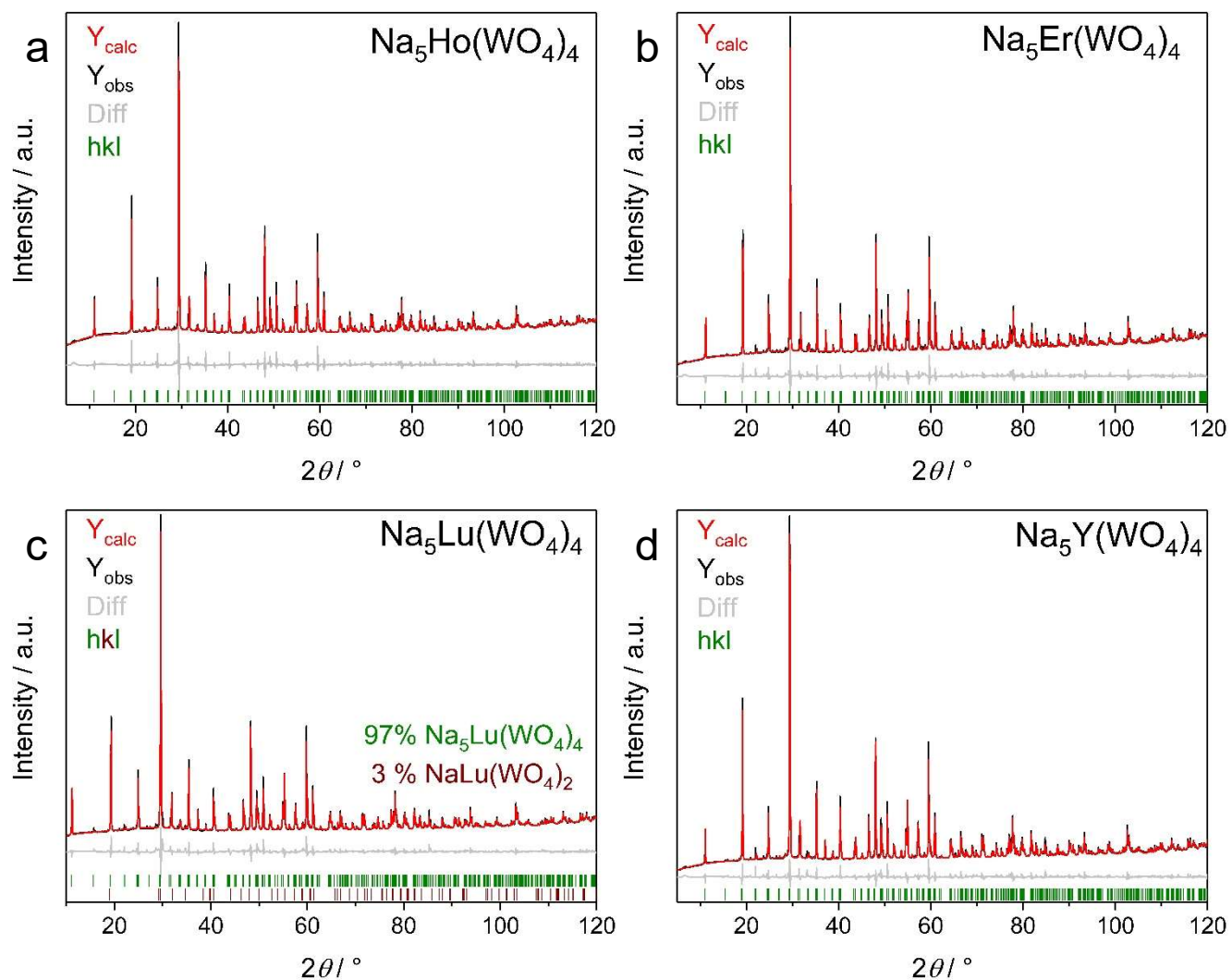


Fig. S4: Rietveld refinements of (a) $\text{Na}_5\text{Ho}(\text{WO}_4)_4$, (b) $\text{Na}_5\text{Er}(\text{WO}_4)_4$, (c) $\text{Na}_5\text{Lu}(\text{WO}_4)_4$ and (d) $\text{Na}_5\text{Y}(\text{WO}_4)_4$ prepared by flux synthesis; further details can be found in Table S4.

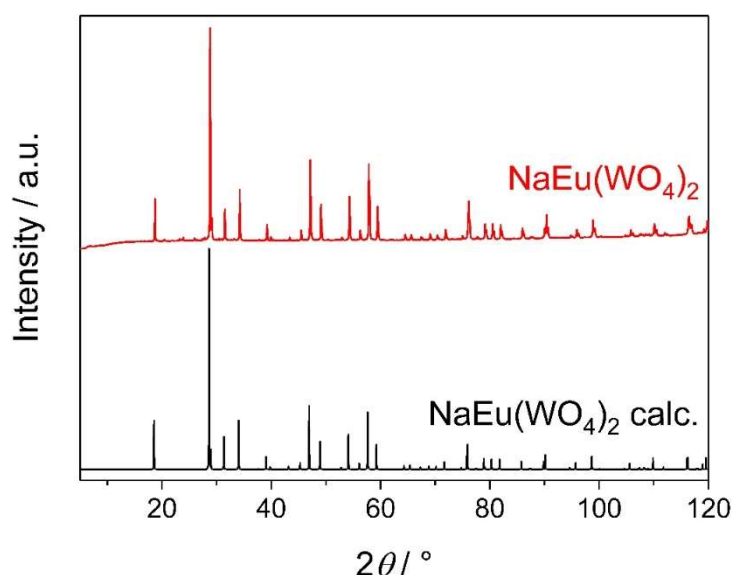


Fig. S5: Powder XRD pattern of polycrystalline $\text{NaEu}(\text{WO}_4)_2$ compared to a pattern calculated from single crystal data (see Table 1 and S1) showing phase purity.

Table S5. Selected interatomic distances (in pm) and angles (in deg) of $\text{NaEu}(\text{WO}_4)_2$ ^a

Na/Eu–O ^b	245.71(18); 247.67(18)
$\sum \text{IR} (\text{Na/Eu–O})^1$ ^c	248
Na/Eu–Na/Eu	388.03(1)
W–O	178.97(18)
$\sum \text{IR} (\text{W–O})^1$	178
O–W–O	107.13(6); 114.26(12)

^a The respective standard deviations are given in parentheses; ^b There are two groups of four oxygen in different distances to cation; ^c The average value of Na^+ and Eu^{3+} was used for the sum of ionic radii.

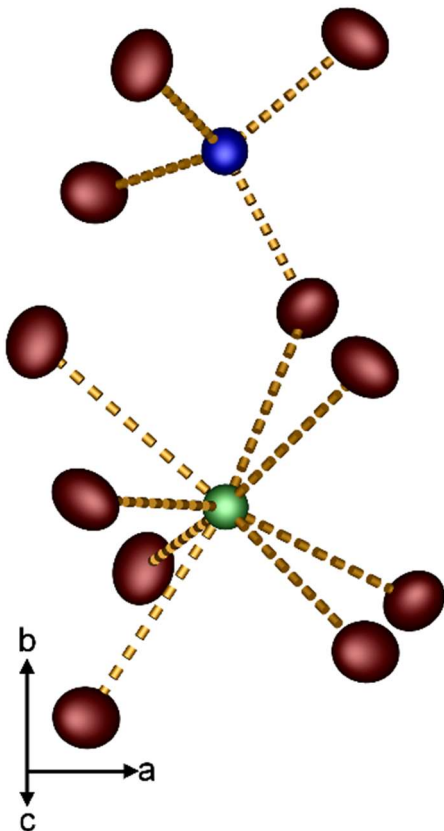


Fig. S6: Coordination environments of $\text{Na}^+/\text{Eu}^{3+}$ (green) and W^{6+} (blue) in $\text{NaEu}(\text{WO}_4)_2$: The former form $[(\text{Na}/\text{Eu})\text{O}_8]$ dodecahedra and the latter WO_4 tetrahedra; oxygen is depicted in red; the ellipsoids are shown at 90% probability.

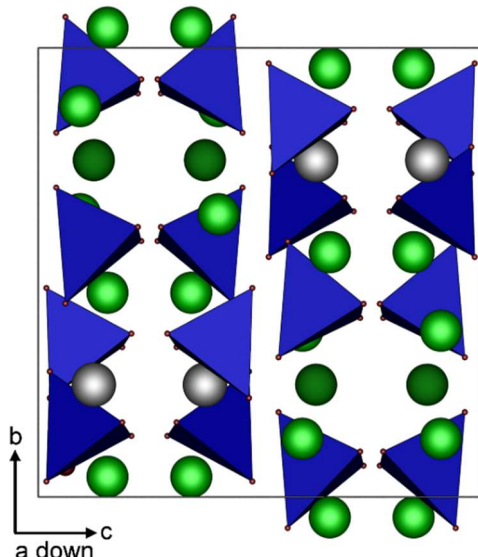


Fig. S7: The unit cell of $\text{Na}_5\text{M}(\text{WO}_4)_4$ with blue WO_4 tetrahedra, green $\text{Na}(1)$, dark green $\text{Na}(2)$) and grey M^{3+}

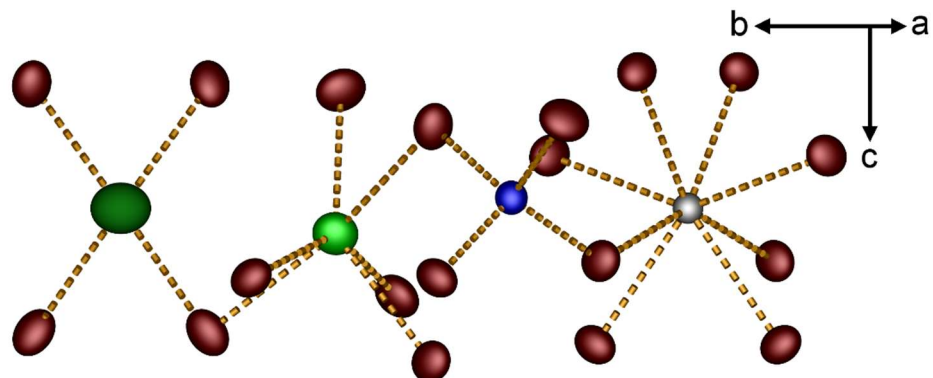


Fig. S8: Coordination environments of Na^+ (light green $\text{Na}(1)$ and dark green $\text{Na}(2)$) Eu^{3+} (grey) and W^{6+} (blue) in $\text{Na}_5\text{Eu}(\text{WO}_4)_4$: they form $\text{Na}(1)\text{O}_6$ trigonal prisms, $\text{Na}(2)\text{O}_4$ tetrahedra, WO_4 tetrahedra and EuO_8 dodecahedra together with oxygen (red), respectively; the ellipsoids are shown at 90% probability.

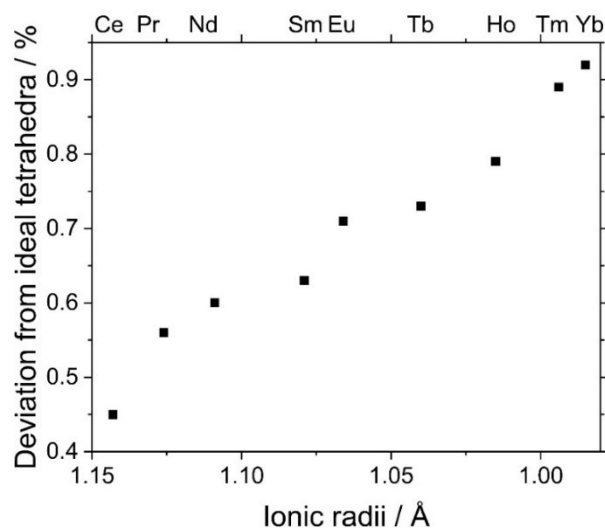


Fig. S9: The WO_4 tetrahedra's deviation from the tetrahedral symmetry calculated by the method of Balic-Zunic² and Makovicky³ is increasing with decreasing ionic radii of M^{3+} in $\text{Na}_5\text{M}(\text{WO}_4)_4$.

Table S6. Selected interatomic distances (in pm), angles (in deg) and the deviation from the ideal symmetry Δ_{octa} or Δ_{tetr} (in %) of $\text{Na}_5M(\text{WO}_4)_4$ ($M = \text{La}, \text{Ce}, \text{Pr}, \text{Nd}, \text{Sm}$)^a

	$\text{Na}_5\text{La}(\text{WO}_4)_4$	$\text{Na}_5\text{Ce}(\text{WO}_4)_4$	$\text{Na}_5\text{Pr}(\text{WO}_4)_4$	$\text{Na}_5\text{Nd}(\text{WO}_4)_4$	$\text{Na}_5\text{Sm}(\text{WO}_4)_4$
Data	Rietveld	SC-XRD	SC-XRD	SC-XRD	SC-XRD
$M-\text{O}$ ^b	238(1)–247(1)	246.3(7)–247.1(7)	245.4(2)–245.8(2)	244.5(3)–244.7(3)	241.4(2)–241.9(2)
$\sum \text{IR}(M-\text{O})^1$	252	250.3	248.6	246.9	243.9
$M-M$	649.31(1)	646.98(1)	646.07(1)	645.20(2)	642.73(2)
$\text{Na}(1)-\text{O}$	217(1)–275(1)	228.2(8)–257.7(9)	228.7(2)–255.8(2)	229.1(3)–255.2(3)	228.7(2)–253.1(2)
$\sum \text{IR}(\text{Na}(1)-\text{O})^1$ ^c			238; 240		
$\Delta_{\text{octa}}(\text{Na}(1)\text{O}_6)$ ^d	2.00	2.14	2.34	2.79	
$\text{Na}(2)-\text{O}$	239(1)	247.6(8)	246.3(2)	246.4(3)	245.5(2)
$\sum \text{IR}(\text{Na}(2)-\text{O})^1$ ^c			237		
$\Delta_{\text{tetr}}(\text{Na}(2)\text{O}_4)$ ^d	7.39	7.18	7.33	7.40	
$\text{W}-\text{O}$	170(1)–191(1)	176.5(7)–180.2(7)	175.6(2)–180.5(2)	175.6(3)–180.0(3)	175.9(2)–180.6(2)
$\sum \text{IR}(\text{W}-\text{O})^1$ ^c			178; 180		
$\text{O}-\text{W}-\text{O}$	103.0(6)–116.2(5)	106.5(3)–113.3(3)	106.2(1)–113.4(1)	105.9(1)–113.5(1)	105.9(1)–113.7(1)
$\Delta_{\text{tetr}}(\text{WO}_4)$ ^d	-	0.45	0.56	0.6	0.63
$\text{M}-\text{O}-\text{W}$	130.9(6)–137.0(6)	129.1(3)–130.4(4)	129.3(1)–130.2(1)	129.4(2)–130.3(1)	129.3(1)–130.3(1)

^a The respective standard deviations are given in parentheses. The standard deviations from Rietveld refinement are numerical standard deviations as obtained from the refinement and do not necessarily represent an interval of trust.; ^b There are two distinct pairs of $M-\text{O}$ distances. ^c Different sums of ionic radii due to oxygen with both CN = 3 and 4. ^d The deviation of the NaO_6 octahedra, NaO_4 tetrahedra and WO_4 tetrahedra from the ideal symmetry Δ_{octa} or Δ_{tetr} was calculated by the Balic-Zunic² and Makovicky³ for all structures derived from single-crystal XRD data.

Table S7. Selected interatomic distances (in pm), angles (in deg) and deviation from the ideal symmetry Δ_{octa} or Δ_{tetr} (in %) of $\text{Na}_5M(\text{WO}_4)_4$ ($M = \text{Eu}, \text{Gd}, \text{Tb}, \text{Dy}, \text{Ho}$)^a

	$\text{Na}_5\text{Eu}(\text{WO}_4)_4$	$\text{Na}_5\text{Gd}(\text{WO}_4)_4$	$\text{Na}_5\text{Tb}(\text{WO}_4)_4$	$\text{Na}_5\text{Dy}(\text{WO}_4)_4$	$\text{Na}_5\text{Ho}(\text{WO}_4)_4$
Data	SC-XRD	SC-XRD	SC-XRD	Rietveld	SC-XRD
$M-\text{O}$ ^b	240.3(2)–240.7(2)	239.2(2)–239.2(2)	238.2(3)–238.8(3)	222(2)–238(2)	236.0(2)–237.1(2)
$\sum \text{IR} (M-\text{O})^1$	242.6	241.3	240	238.7	237.5
$M-M$	641.81(2)	640.20(2)	640.13(2)	639.32(1)	638.47(2)
$\text{Na}(1)-\text{O}$	229.3(2)–252.3(2)	228.9(2)–251.2(3)	229.6(3)–250.7(3)	226(2)–265(2)	229.6(3)–249.6(3)
$\sum \text{IR} (\text{Na}(1)-\text{O})^1$ ^c			238; 240		
$\Delta_{\text{octa}} (\text{Na}(1)\text{O}_6)$ ^d	2.97	3.33	3.78		3.97
$\text{Na}(2)-\text{O}$	245.0(2)	245.0(2)	244.9(3)	242(2)	243.9(2)
$\sum \text{IR} (\text{Na}(2)-\text{O})^1$			237		
$\Delta_{\text{tetr}} (\text{Na}(2)\text{O}_4)$ ^d	7.53	7.48	7.67		7.81
$\text{W}-\text{O}$	175.6(2)–180.7(2)	175.6(2)–181.0(2)	175.4(3)–180.6(3)	170(2)–191(2)	175.6(2)–180.6(2)
$\sum \text{IR} (\text{W}-\text{O})^1$ ^c			178; 180		
$\text{O}-\text{W}-\text{O}$	105.6(1)–113.8(1)	107.1(1)–113.7(1)	105.5(1)–113.8(1)	97.7(9)–115.9(8)	105.3(1)–114.0(1)
$\Delta_{\text{tetr}} (\text{WO}_4)$ ^d	0.71	0.75	0.73		0.79
$M-\text{O}-\text{W}$	129.4(1)–130.1(1)	129.4(1)–130.0(1)	129.5(1)–130.2(1)	133(1)–133.5(9)	129.5(1)–130.0(1)

^a The respective standard deviations are given in parentheses. The standard deviations from Rietveld refinement are numerical standard deviations as obtained from the refinement and do not necessarily represent an interval of trust.; ^b There are two distinct pairs of M -O distances. ^c Different sums of ionic radii due to oxygen with both CN = 3 and 4. ^d The deviation of the NaO_6 octahedra, NaO_4 tetrahedra and WO_4 tetrahedra from the ideal symmetry Δ_{octa} or Δ_{tetr} was calculated by the Balic-Zunic² and Makovicky³ for all structures derived from single-crystal XRD data.

Table S8. Selected interatomic distances (in pm), angles (in deg) and deviation from the ideal symmetry Δ_{octa} or Δ_{tetra} (in %) of $\text{Na}_5M(\text{WO}_4)_4$ ($M = \text{Er}, \text{Tm}, \text{Yb}$)^a

	$\text{Na}_5\text{Er}(\text{WO}_4)_4$	$\text{Na}_5\text{Tm}(\text{WO}_4)_4$	$\text{Na}_5\text{Yb}(\text{WO}_4)_4$
Data	Rietveld	SC-XRD	SC-XRD
$M-\text{O}^b$	232(1)–243(1)		233.3(3)–234.7(3)
$\sum \text{IR } (M-\text{O})^1$	236.4	235.4	234.5
$M-M$	637.59(1)	636.14(3)	635.93(5)
$\text{Na}(1)-\text{O}$	208(1)–264(2)	228.9(3)–247.7(3)	229.6(3)–247.2(3)
$\sum \text{IR } (\text{Na}(1)-\text{O})^1$ ^c		238; 240	
$\Delta_{\text{octa}} (\text{Na}(1)\text{O}_6)$ ^d		4.53	4.37
$\text{Na}(2)-\text{O}$	228(2)	243.1(2)	243.5(3)
$\sum \text{IR } (\text{Na}(2)-\text{O})^1$		237	
$\Delta_{\text{tetra}} (\text{Na}(2)\text{O}_4)$ ^d		7.77	8.01
$\text{W}-\text{O}$	170(1)–191(2)	175.3(2)–181.0(2)	175.7(3)–181.0(3)
$\sum \text{IR } (\text{W}-\text{O})^1$ ^c		178; 180	
$\text{O}-\text{W}-\text{O}$	98.6(7)–116.5(7)	105.2(1)–114.1(1)	104.9(1)–114.3(1)
$\Delta_{\text{tetra}} (\text{WO}_4)$ ^d	-	0.89	0.92
$M-\text{O}-\text{W}$	130.7(7)–131.7(8)	129.4(1)–129.9(1)	129.3(1)–129.6(1)

^a The respective standard deviations are given in parentheses. The standard deviations from Rietveld refinement are numerical standard deviations as obtained from the refinement and do not necessarily represent an interval of trust.; ^b There are two distinct pairs of M-O distances. ^cDifferent sums of ionic radii due to oxygen with both CN = 3 and 4. ^d The deviation of the NaO_6 octahedra, NaO_4 tetrahedra and WO_4 tetrahedra from the ideal symmetry Δ_{octa} or Δ_{tetra} was calculated by the method of Balic-Zunic² and Makovicky³ for all structures derived from single-crystal XRD data.

Table S9. Selected interatomic distances (in pm), angles (in deg) and deviation from the ideal symmetry Δ_{octa} or Δ_{tetra} (in %) of $\text{Na}_5M(\text{WO}_4)_4$ ($M = \text{Lu}, \text{Y}, \text{Bi}$)^a

	$\text{Na}_5\text{Lu}(\text{WO}_4)_4$	$\text{Na}_5\text{Y}(\text{WO}_4)_4$	$\text{Na}_5\text{Bi}(\text{WO}_4)_4$
Data	Rietveld	Rietveld	SC-XRD
$M-\text{O}^b$	226(1)–238(1)	228(1)–243(1)	243.7(4)–244.5(4)
$\sum \text{IR } (M-\text{O})^1$	233.7	237.9	234.5
$M-M$	635.39(1)	638.23(1)	643.85(2)
$\text{Na}(1)-\text{O}$	212(2)–269(2)	218(1)–258(2)	228.8(4)–253.4(4)
$\sum \text{IR } (\text{Na}(1)-\text{O})^1$ ^c		238; 240	
$\Delta_{\text{octa}} (\text{Na}(1)\text{O}_6)$ ^d		2.17	
$\text{Na}(2)-\text{O}$	237(2)	242(1)	245.8(4)
$\sum \text{IR } (\text{Na}(2)-\text{O})^1$		237	
$\Delta_{\text{tetra}} (\text{Na}(2)\text{O}_4)$ ^d		7.49	
$\text{W}-\text{O}$	172(1)–190(1)	164(1)–189(1)	175.3(4)–180.5(4)
$\sum \text{IR } (\text{W}-\text{O})^1$ ^c		178; 180	
$\text{O}-\text{W}-\text{O}$	98.5(7)–119.8(6)	99.8(6)–114.6(5)	105.3(2)–114.1(2)
$\Delta_{\text{tetra}} (\text{WO}_4)$ ^d	-	-	0.71
$M-\text{O}-\text{W}$	130.2(7)–131.2(7)	130.2(6)–135.2(6)	128.5(2)–129.3(2)

^a The respective standard deviations are given in parentheses. The standard deviations from Rietveld refinement are numerical standard deviations as obtained from the refinement and do not necessarily represent an interval of trust.; ^b There are two distinct pairs of M-O distances. ^cDifferent sums of ionic radii due to oxygen with both CN = 3 and 4. ^d The deviation of the NaO_6 octahedra, NaO_4 tetrahedra and WO_4 tetrahedra from the ideal symmetry Δ_{octa} or Δ_{tetra} was calculated by the method of Balic-Zunic² and Makovicky³ for all structures derived from single-crystal XRD data.

$i\bar{4}_1/a$	NaEu $(WO_4)_2$	Na1/Eu1 4a 0 1/4 1/8	W1 4b 0 1/4 5/8	O1 16f 0.2413 0.0971 0.5398						
$i\bar{5}$ $a+2b, -2a+b, c$ $1/5(x+2y)+1/2, 1/5(-2x+y), z;$ $\pm(2/5, 1/5, 0)$										
		4a 0 1/4 1/8	16f 3/5 0.05 1/8	4b 0 1/4 5/8	16f 3/5 0.05 5/8	16f 0.5871 0.9229 0.5398	16f 0.9871 0.1229 0.5398	16f 0.3871 0.3229 0.5398	16f 0.7871 0.5229 0.5398	16f 0.1871 0.7229 0.5398
$i\bar{4}_1/a$										
Na $_5Eu(WO_4)_4$		Eu1 4a 0 1/4 1/8	Na1 16f 0.6203 0.0452 0.1558	Na2 4b 0 1/4 5/8	W1 16f 0.5944 0.0680 0.6378	O1 16f 0.5296 0.8987 0.2758	O2 16f 0.8199 0.0346 0.4817	O3 16f 0.3861 0.3111 0.5405	O4 16f 0.8190 0.3338 0.1889	

Fig. S10: Group–subgroup scheme in the Bärnighausen formalism^{4,5} showing the symmetry relation between Na $_5Eu(WO_4)_4$ and NaEu $(WO_4)_2$.

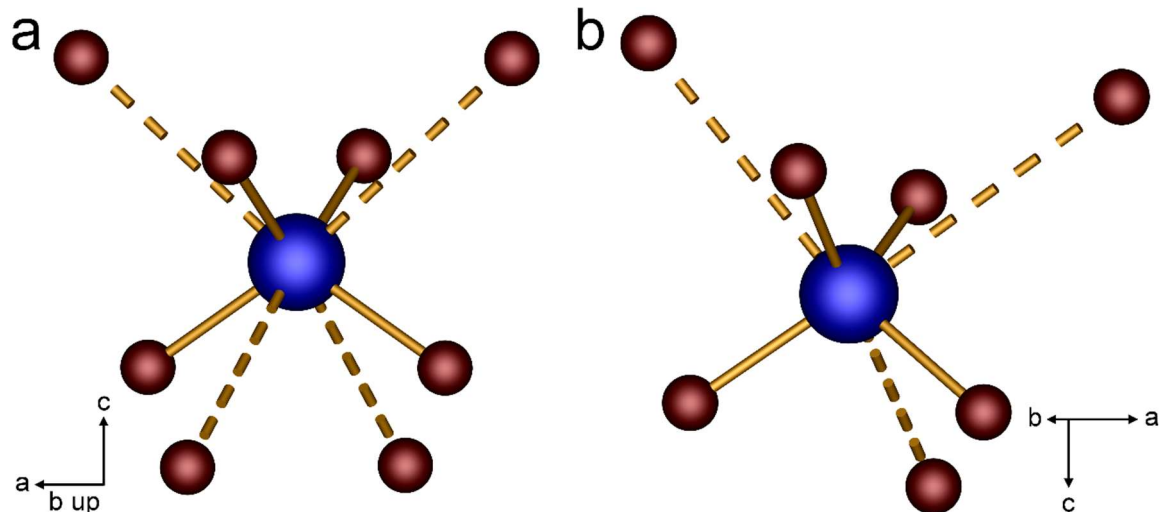


Fig. S11: Coordination environments of W $^{6+}$ (blue) in (a) NaEu $(WO_4)_2$ and (b) Na $_5Eu(WO_4)_4$: they differ in the second coordination sphere; the WO $_4$ tetrahedra in the first coordination sphere are tetracapped and tricapped in the second coordination sphere, respectively; oxygen is depicted in red, tungsten in blue.

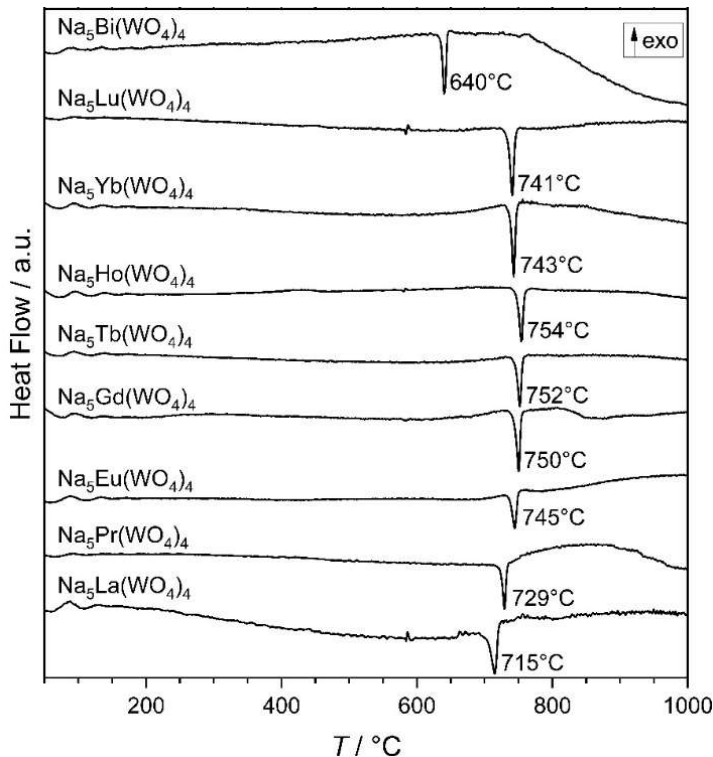


Fig. S12: DSC signals of $\text{Na}_5\text{M}(\text{WO}_4)_4$ ($\text{M} = \text{La, Pr, Eu, Gd, Tb, Ho, Yb, Lu, Bi}$): all samples show one endothermic peak related to the simultaneous melting and decomposition point labelled with the temperature of the peaks' maxima (T_d).

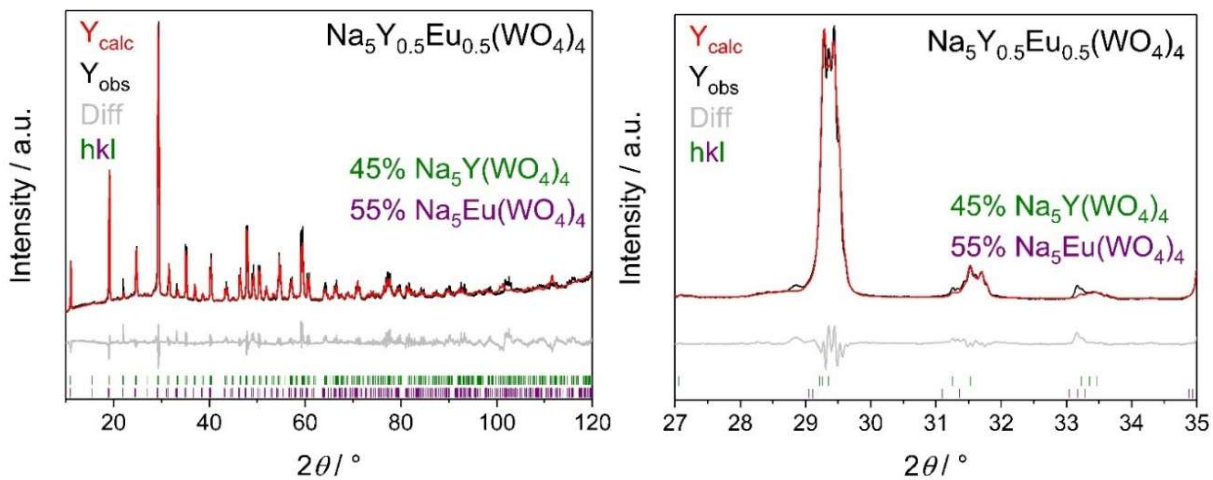


Fig. S13: Rietveld refinement of $\text{Na}_5\text{Y}_{0.5}\text{Eu}_{0.5}(\text{WO}_4)_4$ prepared via the flux synthesis with 500% Na_2WO_4 surplus showing a phase mixture of 45% $\text{Na}_5\text{Y}(\text{WO}_4)_4$ and 55% $\text{Na}_5\text{Eu}(\text{WO}_4)_4$: details can be found in Table S12; the enlarged depiction on the right shows the splitting of the main reflection at $2\theta \approx 29.5^\circ$.

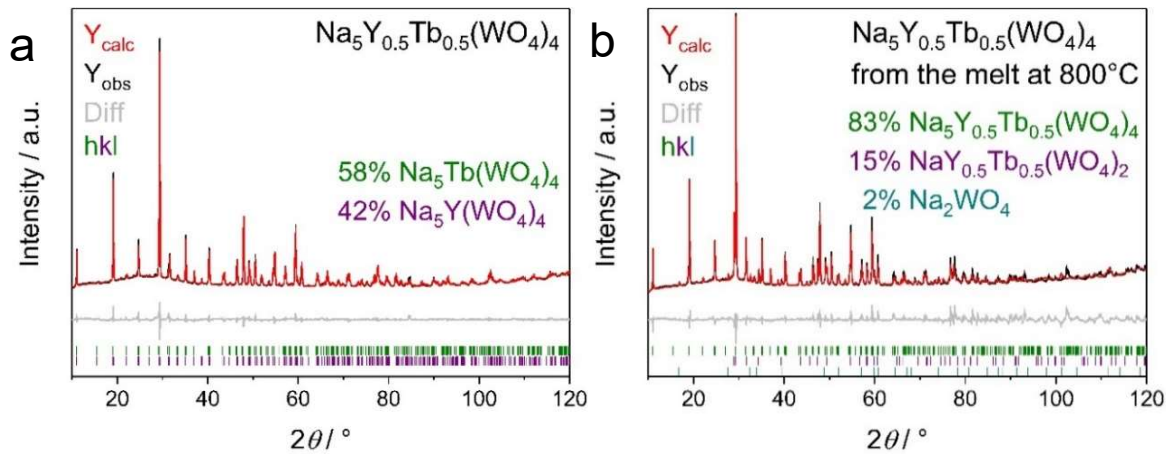


Fig. S14: (a) Rietveld refinement of $\text{Na}_5\text{Y}_{0.5}\text{Tb}_{0.5}(\text{WO}_4)_4$ prepared via the synthesis with 500% Na_2WO_4 surplus showing a phase mixture of 58% $\text{Na}_5\text{Y}(\text{WO}_4)_4$ and 42% $\text{Na}_5\text{Eu}(\text{WO}_4)_4$ and (b) of $\text{Na}_5\text{Y}_{0.5}\text{Tb}_{0.5}(\text{WO}_4)_4$ after subsequent melting at 800°C in a Pt crucible showing a phase mixture of 83% $\text{Na}_5\text{Y}_{0.5}\text{Tb}_{0.5}(\text{WO}_4)_4$, 15% $\text{NaY}_{0.5}\text{Tb}_{0.5}(\text{WO}_4)_2$ and 2% Na_2WO_4 : details can be found in Table S12.

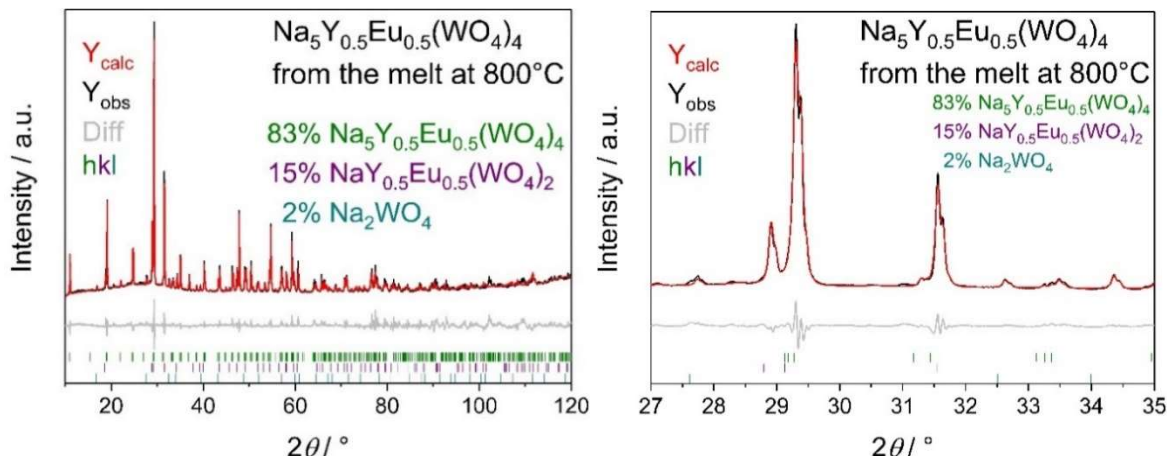


Fig. S15: Rietveld refinement of $\text{Na}_5\text{Y}_{0.5}\text{Eu}_{0.5}(\text{WO}_4)_4$ prepared via the synthesis with 500% Na_2WO_4 surplus and subsequently melted at 800°C in a Pt crucible showing a phase mixture of 83% $\text{Na}_5\text{Y}_{0.5}\text{Eu}_{0.5}(\text{WO}_4)_4$, 15% $\text{NaY}_{0.5}\text{Eu}_{0.5}(\text{WO}_4)_2$ and 2% Na_2WO_4 : details can be found in Table S12; the enlarged depiction on the right shows the non-splitting of the main reflection at $2\theta \approx 29.5^\circ$.

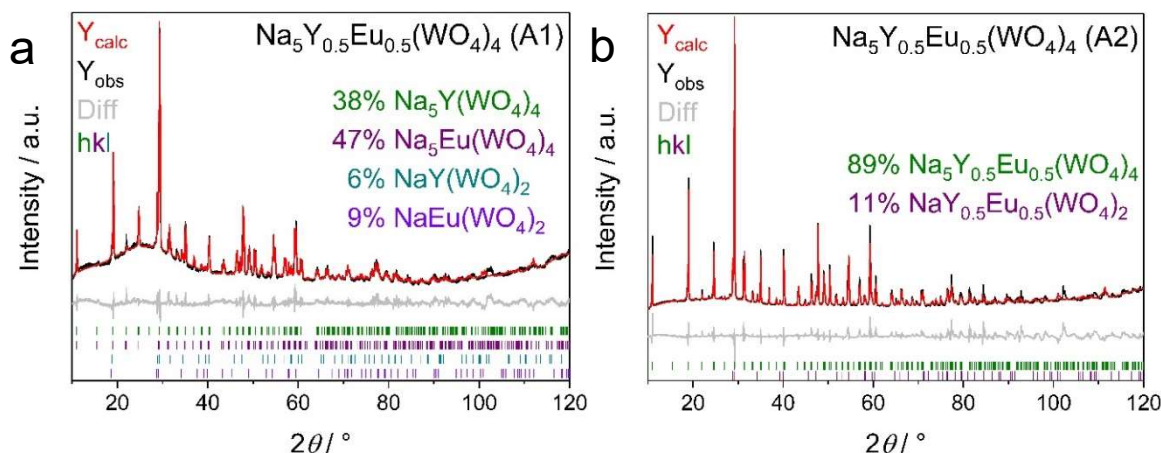


Fig. S16: Rietveld refinement of $\text{Na}_5\text{Y}_{0.5}\text{Eu}_{0.5}(\text{WO}_4)_4$ prepared via solid state syntheses A1 (a) and A2 (b): The product of synthesis A1 consists of a phase mixture of 38% $\text{Na}_5\text{Y}(\text{WO}_4)_4$, 47% $\text{Na}_5\text{Eu}(\text{WO}_4)_4$, 6% $\text{NaY}(\text{WO}_4)_2$ and 9% $\text{NaEu}(\text{WO}_4)_2$, while the sample prepared via A2 shows only two phases of 89% $\text{Na}_5\text{Y}_{0.5}\text{Eu}_{0.5}(\text{WO}_4)_4$ and 11% $\text{NaY}_{0.5}\text{Eu}_{0.5}(\text{WO}_4)_2$; details can be found in Table S12.

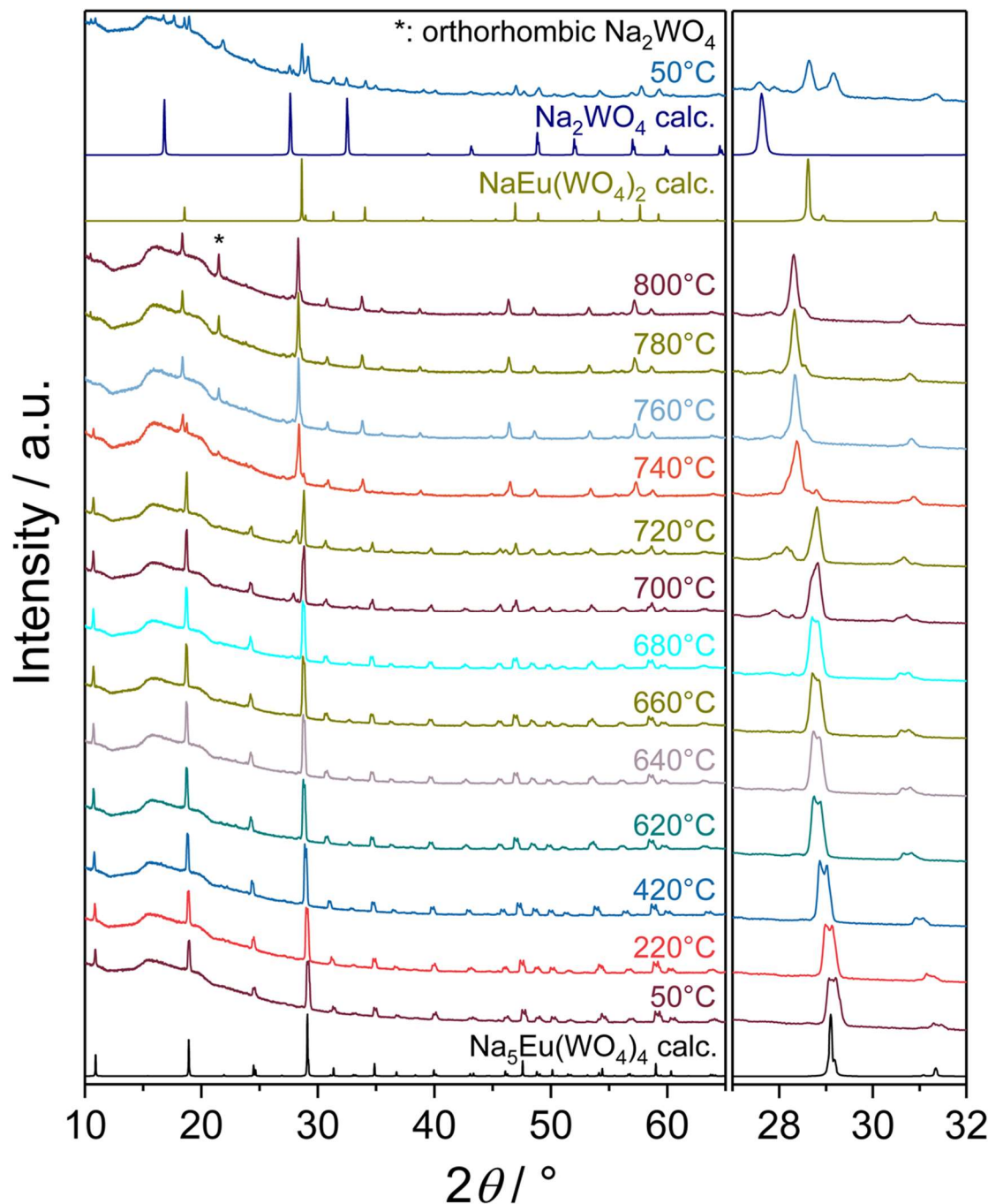


Fig. S17: Variable temperature powder XRD patterns of $\text{Na}_5\text{Y}_{0.5}\text{Eu}_{0.5}(\text{WO}_4)_4$ prepared via the flux synthesis with 500% Na_2WO_4 surplus compared to theoretical patterns calculated from the single crystal data for $\text{Na}_5\text{Eu}(\text{WO}_4)_4$ and $\text{NaEu}(\text{WO}_4)_2$ plus from literature for Na_2WO_4 .⁶ The patterns show the closing of the miscibility gap between 680°C and 720°C with the double reflection around $2\theta=29^\circ$ becoming a single reflection as well as the decomposition into $\text{NaY}_{0.5}\text{Eu}_{0.5}(\text{WO}_4)_2$ and Na_2WO_4 starting around 700°C; moreover, the reflexes related to Na_2WO_4 disappear above 720°C due to the melting of this phase; there is an experimental offset between the furnace temperatures displayed in the graph and the actual temperature at the sample of approximately 20°C; the additional reflection at $2\theta=21.5^\circ$ marked with a black asterisk could be assigned to the orthorhombic high-temperature modification of Na_2WO_4 reported by Pistorius.⁷

Table S10. Structural data from the Rietveld refinement on $\text{Na}_5\text{Y}_{1-x}\text{Eu}_x(\text{WO}_4)_4$ and $\text{Na}_5\text{Y}_{1-y}\text{Tb}_y(\text{WO}_4)_4$ ^{a, b}

	$\text{Na}_5\text{Y}_{0.5}\text{Eu}_{0.5}(\text{WO}_4)_4$	$\text{Na}_5\text{Y}_{0.5}\text{Eu}_{0.5}(\text{WO}_4)_4 \text{ M}^c$	$\text{Na}_5\text{Y}_{0.5}\text{Eu}_{0.5}(\text{WO}_4)_4$ (A1)	$\text{Na}_5\text{Y}_{0.5}\text{Eu}_{0.5}(\text{WO}_4)_4$ (A2)	$\text{Na}_5\text{Y}_{0.5}\text{Tb}_{0.5}(\text{WO}_4)_4$	$\text{Na}_5\text{Y}_{0.5}\text{Tb}_{0.5}(\text{WO}_4)_4 \text{ M}^c$
R_{wp}	0.04434	0.04029	0.02439	0.05042	0.02004	0.04092
No. of independent parameters	44	42	49	43	45	46
Temperature / K	300(3)					
Radiation; wavelength λ / Å	CuK α ; 1.54184					
Diffractometer	Seifert 3003 TT					
2θ range / deg	5–120					
First Phase	$\text{Na}_5\text{Y}(\text{WO}_4)_4$	$\text{Na}_5\text{Y}_{0.5}\text{Eu}_{0.5}(\text{WO}_4)_4$	$\text{Na}_5\text{Y}(\text{WO}_4)_4$	$\text{Na}_5\text{Y}_{0.5}\text{Eu}_{0.5}(\text{WO}_4)_4$	$\text{Na}_5\text{Y}(\text{WO}_4)_4$	$\text{Na}_5\text{Y}_{0.5}\text{Tb}_{0.5}(\text{WO}_4)_4$
Fraction of first phase / wt.-%	45	83	38	89	42	83
a / pm	1143.70(2)	1146.879(14)	1143.60(2)	1146.315(17)	1143.562(16)	1145.023(18)
c / pm	1134.14(3)	1137.303(15)	1134.40(4)	1138.78(2)	1133.83(2)	1135.50(2)
Volume / 10^6 pm ³	1483.50(7)	1495.93(4)	1483.58(8)	1496.40(6)	1482.75(5)	1488.73(6)
R_{Bragg} / %	2.279	2.263	1.088	3.254	1.036	2.224
Second Phase	$\text{Na}_5\text{Eu}(\text{WO}_4)_4$	$\text{NaY}_{0.5}\text{Eu}_{0.5}(\text{WO}_4)_2$	$\text{Na}_5\text{Eu}(\text{WO}_4)_4$	$\text{NaY}_{0.5}\text{Eu}_{0.5}(\text{WO}_4)_2$	$\text{Na}_5\text{Tb}(\text{WO}_4)_4$	$\text{NaY}_{0.5}\text{Tb}_{0.5}(\text{WO}_4)_2$
Fraction of second phase / wt.-%	55	15	47	11	58	15
a / pm	1149.57(2)	523.357(14)	1149.05(2)	522.89(5)	1146.404(15)	521.938(19)
c / pm	1140.25(4)	1133.64(6)	1140.18(4)	1134.2(2)	1136.631(18)	1129.70(8)
Volume / 10^6 pm ³	1506.86(8)	310.51(2)	1505.38(7)	310.10(8)	1493.81(5)	307.75(3)
R_{Bragg} / %	3.033	1.963	1.462	1.995	0.897	1.787
Third phase	Na_2WO_4^d		$\text{NaY}(\text{WO}_4)_2$			Na_2WO_4^d
Fraction of third phase / wt.-%	2		6			2
a / pm	912.80(5)		520.67(4)			913.29(7)
c / pm	912.80(5)		1127.27(15)			913.29(7)
Volume / 10^6 pm ³	760.54(13)		305.60(6)			761.78(17)
R_{Bragg} / %	1.968		1.250			1.543
Forth phase			$\text{NaEu}(\text{WO}_4)_2$			
Fraction of forth phase / wt.-%			9			
a / pm			525.15(3)			
c / pm			1138.43(11)			
Volume / 10^6 pm ³			313.95(4)			
R_{Bragg} / %			1.025			

^a The respective standard deviations are given in parentheses. ^b Unless specified differently, all phases crystallise in space group $I4_1/a$ (No. 88) with $Z = 4$ for all $\text{Na}_5M(\text{WO}_4)_4$ phases and $Z = 2$ for all $\text{NaM}(\text{WO}_4)_2$ phases, respectively. ^c The suffix M symbolises the samples obtained from the melt at 800°C. ^d Na_2WO_4 crystallises in space group $Fd\bar{3}m$ (No. 227) with $Z = 8$.

Table S11. Crystal data and structure refinements of $\text{Na}_5\text{Y}_{0.49}\text{Eu}_{0.51}(\text{WO}_4)_4$ and $\text{Na}_5\text{Y}_{0.49}\text{Tb}_{0.51}(\text{WO}_4)_4$ determined from single-crystal data^a

	$\text{Na}_5\text{Y}_{0.49}\text{Eu}_{0.51}(\text{WO}_4)_4$	$\text{Na}_5\text{Y}_{0.49}\text{Tb}_{0.51}(\text{WO}_4)_4$
CSD-No.	1986865	19868560
$M / \text{g mol}^{-1}$	1228.23	1231.29
Crystal size / mm ³	0.05 × 0.02 × 0.02	0.05 × 0.03 × 0.03
Temperature / K		300(3)
Space group		$I4_1/a$ (No. 88)
a / pm	1146.81(4)	1146.02(2)
c / pm	1137.59(4)	1136.78(3)
Volume / 10 ⁶ pm ³	1496.13(12)	1493.00(7)
Z		4
$\rho_{\text{calcd}} / \text{g cm}^{-3}$	5.45	5.47
Absorption coefficient μ / mm^{-1}	34.9	35.2
$F(000) / e$	2120	2124
Radiation; wavelength $\lambda / \text{\AA}$		$\text{MoK}\alpha$; 0.71073
Diffractometer		Bruker D8 Venture
Absorption correction		Multi-scan
Transmission (min; max)	0.6078; 0.7475	0.4460; 0.7491
Index range $h k l$	-20/20 -20/19 -19/19	-21/21 -21/21 -21/21
θ range / deg	2.522–38.483	2.524–42.492
Reflections collected	26544	20167
Independent reflections	2103	2682
R_{int}	0.0633	0.0221
Obs. reflections ($I > 2 \sigma(I)$)	1822	2438
Refined parameters	61	61
R_1 (all data)	0.0271	0.021
wR_2 (all data)	0.0325	0.0311
GooF	1.054	1.113
Residual electron density (max; min) / e ⁻	1.68; -1.45	1.28; -1.14

^a The respective standard deviations are given in parentheses.

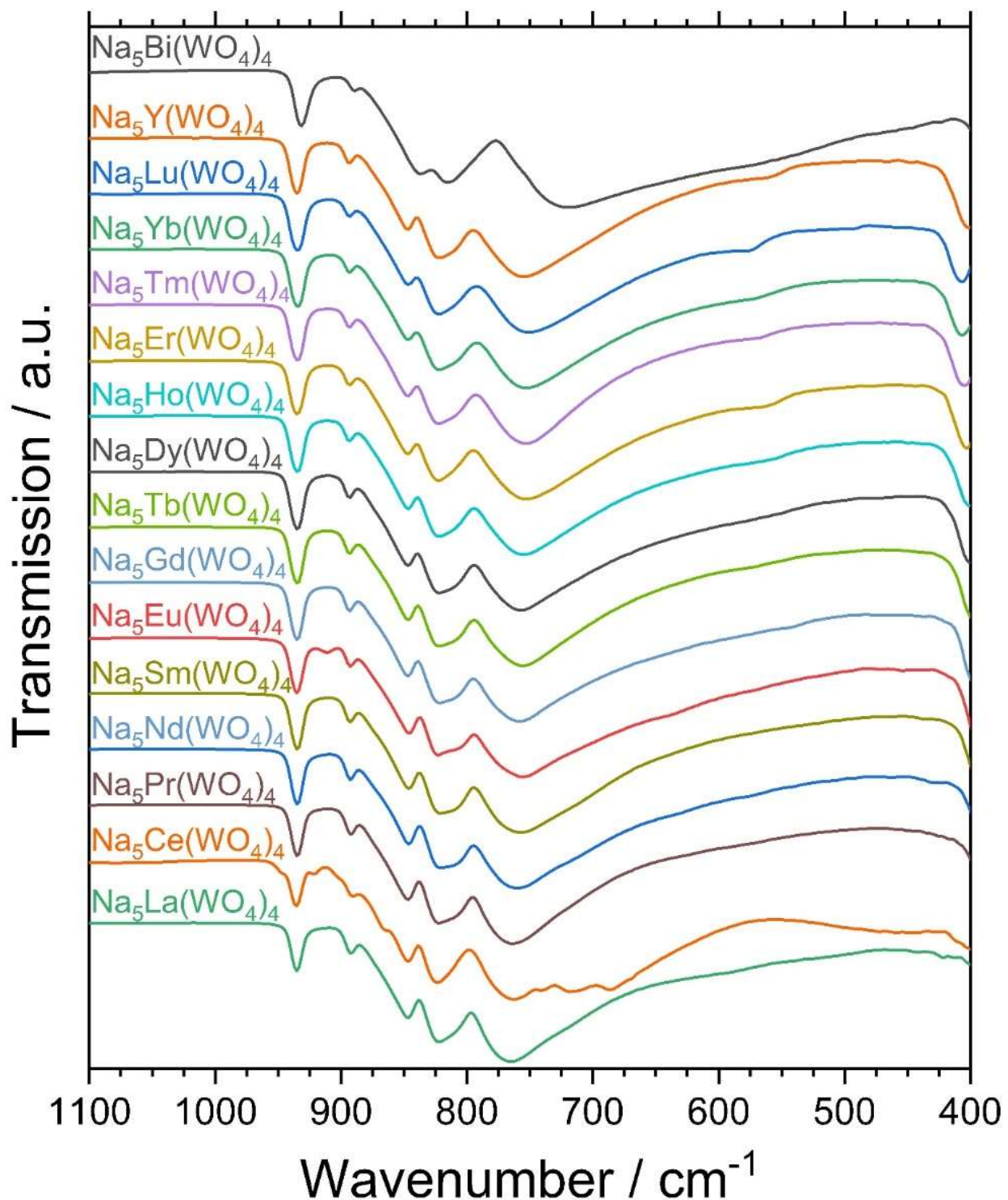


Fig.S18: FTIR spectra of $\text{Na}_5\text{M}(\text{WO}_4)_4$ ($\text{M} = \text{La, Ce, Pr, Nd, Sm, Eu, Gd, Tb, Dy, Ho, Er, Tm, Yb, Lu, Y, Bi}$)

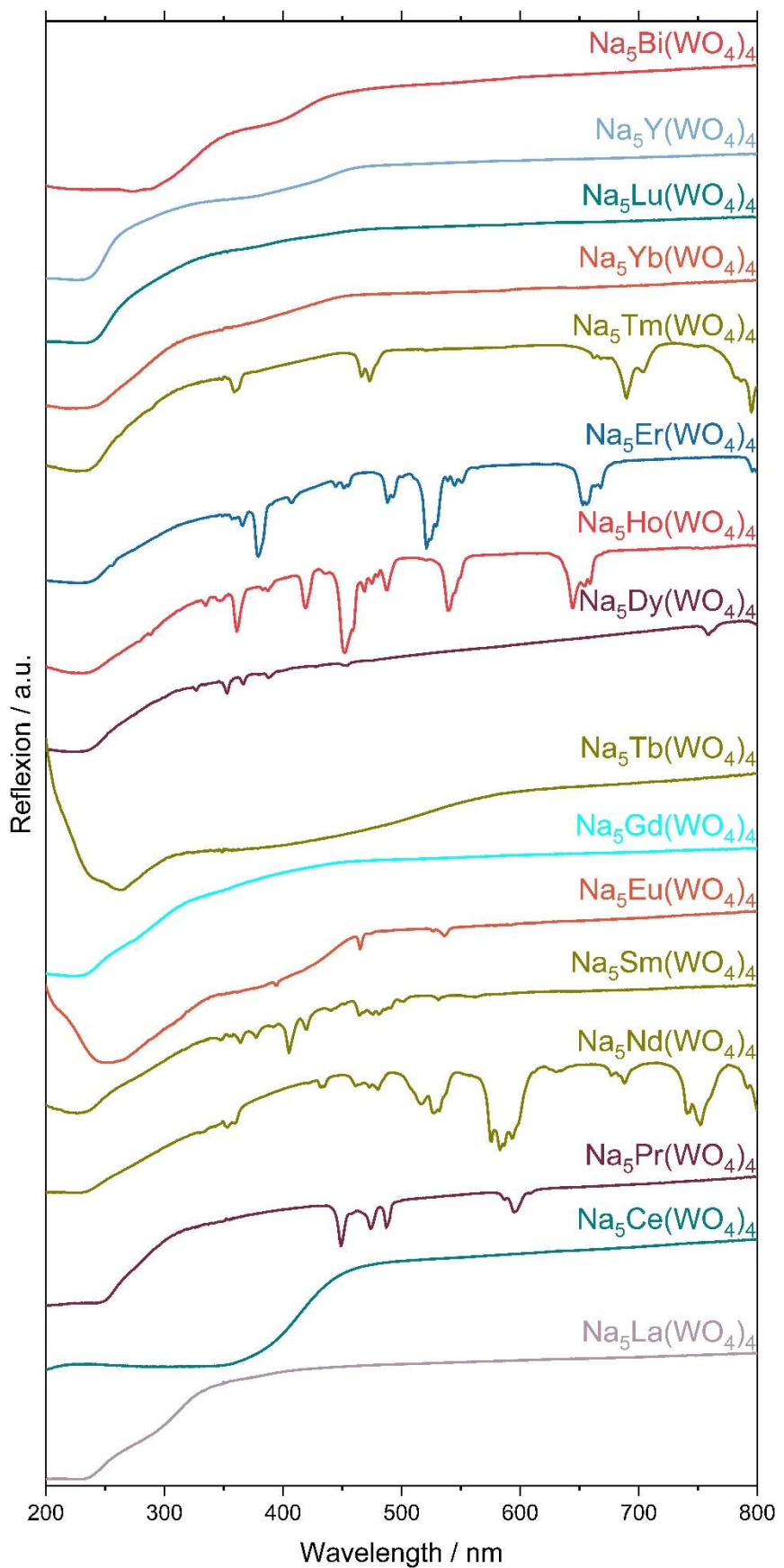


Fig.S19: UV/Vis spectra of $\text{Na}_5\text{M}(\text{WO}_4)_4$ ($\text{M} = \text{La, Ce, Pr, Nd, Sm, Eu, Gd, Tb, Dy, Ho, Er, Tm, Yb, Lu, Y, Bi}$)

Table S12. Assignment of absorption bands in UV/Vis spectra of $\text{Na}_5M(\text{WO}_4)_4$ besides the $\text{O}^{2-}\text{-W}^{6+}$ LMCT found between 230 nm and 250 nm for all samples.^{8,9,10,11,12,13,14,15,16,17,18 a}

$\text{Na}_5\text{Ce}(\text{WO}_4)_4$	Wavelength λ / nm	Energy E / cm^{-1}	Transition
	350	28571	4f-5d
$\text{Na}_5\text{Pr}(\text{WO}_4)_4$	Wavelength λ / nm	Energy E / cm^{-1}	f-f transition
	449	22272	$^3\text{H}_4 \rightarrow ^1\text{I}_6$
	474	21097	$^3\text{H}_4 \rightarrow ^3\text{P}_1$
	487	20534	$^3\text{H}_4 \rightarrow ^3\text{P}_0$
	587	17036	$^3\text{H}_4 \rightarrow ^1\text{D}_2$
	595	16807	$^3\text{H}_4 \rightarrow ^1\text{D}_2$
	609	16420	$^3\text{H}_4 \rightarrow ^1\text{D}_2$
$\text{Na}_5\text{Nd}(\text{WO}_4)_4$	Wavelength λ / nm	Energy E / cm^{-1}	f-f transition
	353	28329	$^4\text{I}_{9/2} \rightarrow ^2\text{I}_{11/2}$
	360	27778	$^4\text{I}_{9/2} \rightarrow ^4\text{D}_{3/2}$
	422	23697	$^4\text{I}_{9/2} \rightarrow ^2\text{D}_{5/2}$
	432; 435	23148	$^4\text{I}_{9/2} \rightarrow ^2\text{P}_{1/2}$
	461	21692	$^4\text{I}_{9/2} \rightarrow ^4\text{G}_{11/2}, (^2\text{D}, ^2\text{F})_{3/2}$
	473	21142	$^4\text{I}_{9/2} \rightarrow ^2\text{G}_{9/2}$
	480	20833	$^4\text{I}_{9/2} \rightarrow ^2\text{K}_{15/2}$
	517	19342	$^4\text{I}_{9/2} \rightarrow ^4\text{G}_{9/2}$
	527; 532	18975	$^4\text{I}_{9/2} \rightarrow ^4\text{G}_{7/2}$
	576; 583, 587	17361	$^4\text{I}_{9/2} \rightarrow ^2\text{G}_{7/2}$
	594	16835	$^4\text{I}_{9/2} \rightarrow ^4\text{G}_{5/2}$
	631	15848	$^4\text{I}_{9/2} \rightarrow ^2\text{H}_{11/2}$
	677, 688	14771	$^4\text{I}_{9/2} \rightarrow ^4\text{F}_{9/2}$
	741	13495	$^4\text{I}_{9/2} \rightarrow ^5\text{S}_{3/2}$
	752	13298	$^4\text{I}_{9/2} \rightarrow ^4\text{F}_{7/2}$
	791	12642	$^4\text{I}_{9/2} \rightarrow ^2\text{H}_{9/2}$
$\text{Na}_5\text{Sm}(\text{WO}_4)_4$	Wavelength λ / nm	Energy E / cm^{-1}	f-f transition
	364	27473	$^6\text{H}_{5/2} \rightarrow ^4\text{D}_{3/2}$
	377	26525	$^6\text{H}_{5/2} \rightarrow ^6\text{P}_{7/2}$
	392	25510	$^6\text{H}_{5/2} \rightarrow ^4\text{L}_{15/2}$
	405	24691	$^6\text{H}_{5/2} \rightarrow ^4\text{L}_{13/2}$
	420	23810	$^6\text{H}_{5/2} \rightarrow (^6\text{P}, ^4\text{P})_{5/2}$
	440	22727	$^6\text{H}_{5/2} \rightarrow ^4\text{G}_{9/2}$
	452	22124	$^6\text{H}_{5/2} \rightarrow ^4\text{F}_{5/2}$
	464	21552	$^6\text{H}_{5/2} \rightarrow ^6\text{I}_{13/2}$

	476	21008	$^6\text{H}_{5/2} \rightarrow ^4\text{I}_{11/2}$
	481	20790	$^6\text{H}_{5/2} \rightarrow ^4\text{M}_{15/2}$
	491	20367	$^6\text{H}_{5/2} \rightarrow ^4\text{I}_{9/2}$
	502	19920	$^6\text{H}_{5/2} \rightarrow ^4\text{G}_{7/2}$
	531	18832	$^6\text{H}_{5/2} \rightarrow ^4\text{F}_{3/2}$
	562	17794	$^6\text{H}_{5/2} \rightarrow ^4\text{G}_{5/2}$
Na ₅ Eu(WO ₄) ₄ ^b	Wavelength λ / nm	Energy E / cm ⁻¹	f-f transition
	395	25316	$^7\text{F}_0 \rightarrow ^5\text{L}_6$
	465; 474	21505	$^7\text{F}_0 \rightarrow ^5\text{D}_2$
	526; 536	19011	$^7\text{F}_0 \rightarrow ^5\text{D}_1$
	579	17271	$^7\text{F}_0 \rightarrow ^5\text{D}_0$
Na ₅ Dy(WO ₄) ₄	Wavelength λ / nm	Energy E / cm ⁻¹	f-f transition
	327	30581	$^6\text{H}_{15/2} \rightarrow ^6\text{P}_{3/2}$
	353	28329	$^6\text{H}_{15/2} \rightarrow ^6\text{P}_{7/2}$
	366	27322	$^6\text{H}_{15/2} \rightarrow ^4\text{M}_{19/2}$
	388	25773	$^6\text{H}_{15/2} \rightarrow ^4\text{I}_{13/2}$
	428	23364	$^6\text{H}_{15/2} \rightarrow ^4\text{G}_{11/2}$
	454	22026	$^6\text{H}_{15/2} \rightarrow ^4\text{I}_{15/2}$
	475	21053	$^6\text{H}_{15/2} \rightarrow ^4\text{F}_{9/2}$
	759	13175	$^6\text{H}_{15/2} \rightarrow ^6\text{F}_{3/2}$
Na ₅ Ho(WO ₄) ₄	Wavelength λ / nm	Energy E / cm ⁻¹	f-f transition
	335	29851	$^5\text{I}_8 \rightarrow (^3\text{F}, ^3\text{H}, ^3\text{G})_4$
	347	28818	$^5\text{I}_8 \rightarrow ^5\text{G}_3$
	361	27701	$^5\text{I}_8 \rightarrow (^5\text{G}, ^3\text{H})_5$
	383	26110	$^5\text{I}_8 \rightarrow ^3\text{K}_7$
	388	25773	$^5\text{I}_8 \rightarrow ^5\text{G}_4$
	419	23867	$^5\text{I}_8 \rightarrow (^5\text{G}, ^3\text{G})_5$
	452	22124	$^5\text{I}_8 \rightarrow ^5\text{F}_1, ^5\text{G}_6$
	469	21322	$^5\text{I}_8 \rightarrow ^3\text{K}_8$
	475	21053	$^5\text{I}_8 \rightarrow ^5\text{F}_2$
	480; 487	20833	$^5\text{I}_8 \rightarrow ^5\text{F}_3$
	540	18519	$^5\text{I}_8 \rightarrow ^5\text{F}_4, ^5\text{S}_2$
	644; 654; 659	15528	$^5\text{I}_8 \rightarrow ^5\text{F}_5$
Na ₅ Er(WO ₄) ₄	Wavelength λ / nm	Energy E / cm ⁻¹	f-f transition
	357	28011	$^4\text{I}_{15/2} \rightarrow ^2\text{G}_{7/2}$
	366	27322	$^4\text{I}_{15/2} \rightarrow ^4\text{G}_{9/2}$

379	26385	$^4I_{15/2} \rightarrow ^4G_{11/2}$
407	24570	$^4I_{15/2} \rightarrow (^2G, ^4F)_{9/2}$
445; 452	22472	$^4I_{15/2} \rightarrow ^4F_{5/2}$
488	20492	$^4I_{15/2} \rightarrow ^4F_{7/2}$
521	19194	$^4I_{15/2} \rightarrow (^2H, ^4G)_{11/2}$
539; 545; 551	18553	$^4I_{15/2} \rightarrow ^4S_{3/2}$
653	15314	$^4I_{15/2} \rightarrow ^4F_{9/2}$
769	13004	$^4I_{15/2} \rightarrow ^4I_{9/2}$
Na₅Tm(WO₄)₄	Wavelength λ / nm	Energy E / cm⁻¹
359	27855	$^3H_6 \rightarrow ^1D_2$
466; 473	21459	$^3H_6 \rightarrow ^1G_4$
662	15106	$^3H_6 \rightarrow ^3F_2$
690; 704	14493	$^3H_6 \rightarrow ^3F_3$
786; 795	12723	$^3H_6 \rightarrow ^3H_4$

^a Doublets and triplets are marked by two or three values in the λ column. Only the respective energy for the first value is displayed. ^b The O²⁻–W⁶⁺ LMCT ($\lambda = 230$ nm) is overlapped with the O²⁻–Eu³⁺ LMCT ($\lambda = 250$ nm).

Table S13. Assignment of emission and excitation peaks in the fluorescence spectra of Na₅M(WO₄)₄.^{8,9,10,13,14,19,20,21,22,23,24,25,26,27,28 a}

Na ₅ Pr(WO ₄) ₄			
Excitation	Wavelength λ / nm	Energy E / cm ⁻¹	Assignment
A	250	40000	O ²⁻ →W ⁶⁺ LMCT
B	446	22422	³ H ₄ → ¹ I ₆
C	470	21277	³ H ₄ → ³ P ₁
D	484	20661	³ H ₄ → ³ P ₀
Emission	Wavelength λ / nm	Energy E / cm ⁻¹	Assignment
	481; 488, 496	20790	³ P ₀ → ³ H ₄
	528	18939	³ P ₁ → ³ H ₅
	546, 553	18315	³ P ₀ → ³ H ₅
	595	16807	¹ D ₂ → ³ H ₄
	616	16234	³ P ₀ → ³ H ₆
	646	15480	³ P ₀ → ³ F ₂
	680	14706	³ P ₀ → ³ F ₃
	730	13699	³ P ₀ → ³ F ₄
Na ₅ Sm(WO ₄) ₄			
Excitation	Wavelength λ / nm	Energy E / cm ⁻¹	Assignment
A	240	41667	O ²⁻ →W ⁶⁺ LMCT
B	304	32895	⁶ H _{5/2} → ⁴ P _{5/2}
C	316	31646	⁶ H _{5/2} → ⁴ P _{3/2}
D	331	30211	⁶ H _{5/2} → ⁴ G _{9/2}
E	344	29070	⁶ H _{5/2} → (⁴ H _{9/2} , ⁴ D _{7/2})
F	362	27624	⁶ H _{5/2} → ⁴ D _{3/2}
G	375	266667	⁶ H _{5/2} → ⁶ P _{7/2}
H	390	25641	⁶ H _{5/2} → ⁴ L _{15/2}
I	403	24814	⁶ H _{5/2} → ⁴ L _{13/2}
J	417	23981	⁶ H _{5/2} → (⁶ P, ⁴ P) _{5/2}
K	439	22779	⁶ H _{5/2} → ⁴ G _{9/2}
L	448	22321	⁶ H _{5/2} → ⁴ F _{5/2}
M	465	21505	⁶ H _{5/2} → ⁶ I _{13/2}
N	471	21231	⁶ H _{5/2} → ⁴ I _{11/2}
O	479	20877	⁶ H _{5/2} → ⁶ M _{15/2}
P	487	20534	⁶ H _{5/2} → ⁴ I _{9/2}
Q	497	20121	⁶ H _{5/2} → ⁴ G _{7/2}
Emission	Wavelength λ / nm	Energy E / cm ⁻¹	Assignment

553; 562	17794	$^4G_{5/2} \rightarrow ^6H_{5/2}$
600	16667	$^4G_{5/2} \rightarrow ^6H_{7/2}$
645; 664	15504	$^4G_{5/2} \rightarrow ^6H_{9/2}$
703	14225	$^4G_{5/2} \rightarrow ^6H_{11/2}$
772	12953	$^4G_{5/2} \rightarrow ^6H_{13/2}$

Na₅Eu(WO₄)₄

Excitation	Wavelength λ / nm	Energy E / cm ⁻¹	Assignment
A	270	37037	O ²⁻ -W ⁶⁺ LMCT + O ²⁻ -Eu ³⁺ LMCT
B	285	35088	$^7F_0 \rightarrow (^5I, ^5H)_6$
C	293	34130	$^7F_0 \rightarrow ^5F_5$
D	298	33557	$^7F_0 \rightarrow ^5F_4$
E	302	33113	$^7F_0 \rightarrow ^5F_2$
F	305	32787	$^7F_0 \rightarrow ^3P_0$
G	317	31546	$^7F_0 \rightarrow ^5H_6$
H	321	31153	$^7F_0 \rightarrow ^5H_7$
I	326	30675	$^7F_0 \rightarrow ^5H_3$
J	361	27701	$^7F_0 \rightarrow ^5D_4$
K	366	27322	$^7F_0 \rightarrow ^5L_3$
L	375	26667	$^7F_0 \rightarrow ^5G_6$
M	380	26316	$^7F_0 \rightarrow ^5L_7$
N	383	26110	$^7F_0 \rightarrow ^5G_2$
O	393; 396; 399	25445	$^7F_0 \rightarrow ^5L_6$
P	415	24096	$^7F_0 \rightarrow ^5D_3$
Q	464; 472, 481, 488	21552	$^7F_0 \rightarrow ^5D_2$
Emission	Wavelength λ / nm	Energy E / cm ⁻¹	Assignment
	535	18692	$^5D_0 \rightarrow ^7F_0$
	591	16920	$^5D_0 \rightarrow ^7F_1$
	606; 611; 615	16502	$^5D_0 \rightarrow ^7F_2$
	653	15314	$^5D_0 \rightarrow ^7F_3$
	693; 699; 702	14430	$^5D_0 \rightarrow ^7F_4$

Na₅Tb(WO₄)₄

Excitation	Wavelength λ / nm	Energy E / cm ⁻¹	Assignment
A	251	39841	O ²⁻ -W ⁶⁺ LMCT + Tb ³⁺ 4f → 5d
B	284	35211	$^7F_6 \rightarrow ^5I_8$
C	295	33898	$^7F_6 \rightarrow ^5H_5$
D	303	33003	$^7F_6 \rightarrow ^5H_6$

E	317	31546	$^7F_6 \rightarrow ^5H_7$
F	326	30675	$^7F_6 \rightarrow ^5D_1$
G	339	29499	$^7F_6 \rightarrow ^5L_7$
H	351	28490	$^7F_6 \rightarrow ^5L_9$
I	358	27933	$^7F_6 \rightarrow ^5G_5$
J	369	27100	$^7F_6 \rightarrow ^5L_{10}$
K	377	26525	$^7F_6 \rightarrow ^5G_6$
Emission	Wavelength λ / nm	Energy E / cm ⁻¹	Assignment
	487; 493	20534	$^5D_4 \rightarrow ^7F_6$
	543; 547	18416	$^5D_4 \rightarrow ^7F_5$
	581; 587	17212	$^5D_4 \rightarrow ^7F_4$
	616; 620	16234	$^5D_4 \rightarrow ^7F_3$
	644; 650	15528	$^5D_4 \rightarrow ^7F_2$
	669	14948	$^5D_4 \rightarrow ^7F_1$
	679	14728	$^5D_4 \rightarrow ^7F_0$
Na ₅ Bi(WO ₄) ₄ ^b			
Excitation	Wavelength λ / nm	Energy E / cm ⁻¹	Assignment
	250; 258	40000	O ²⁻ -W ⁶⁺ LMCT
	273; 275	36630	$^1S_0 \rightarrow ^1P_1$
	281; 290	35587	$^1S_0 \rightarrow ^3P_1$
Emission	Wavelength λ / nm	Energy E / cm ⁻¹	Assignment
	470	21277	$^3P_1 \rightarrow ^1S_0$

^a Doublets, triplets et cetera are marked by two or three values in the λ column. Only the respective energy for the first value is displayed. ^b The two λ values for Na₅Bi(WO₄)₄ represent the maxima at both room temperature and 77 K.

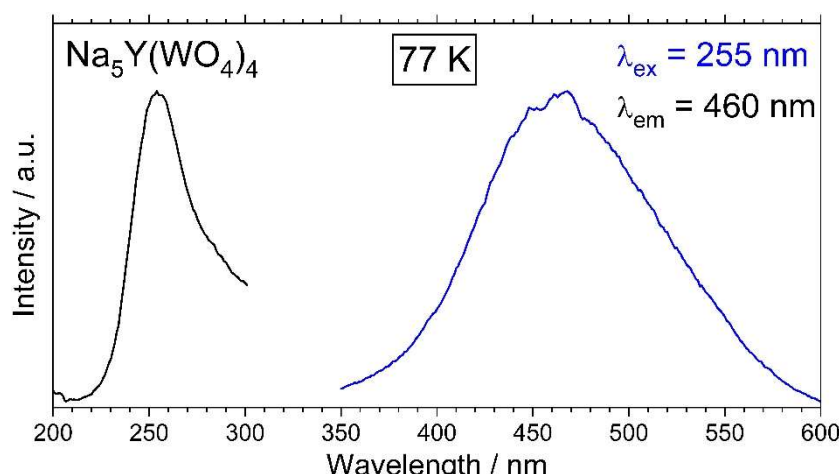


Fig. S20: Excitation and emission spectra of Na₅Y(WO₄)₄ measured at 77 K: the compound shows a broad W⁶⁺-O²⁻ LMCT emission centred at 460 nm; the excitation spectrum was not corrected with respect to the lamp intensity.

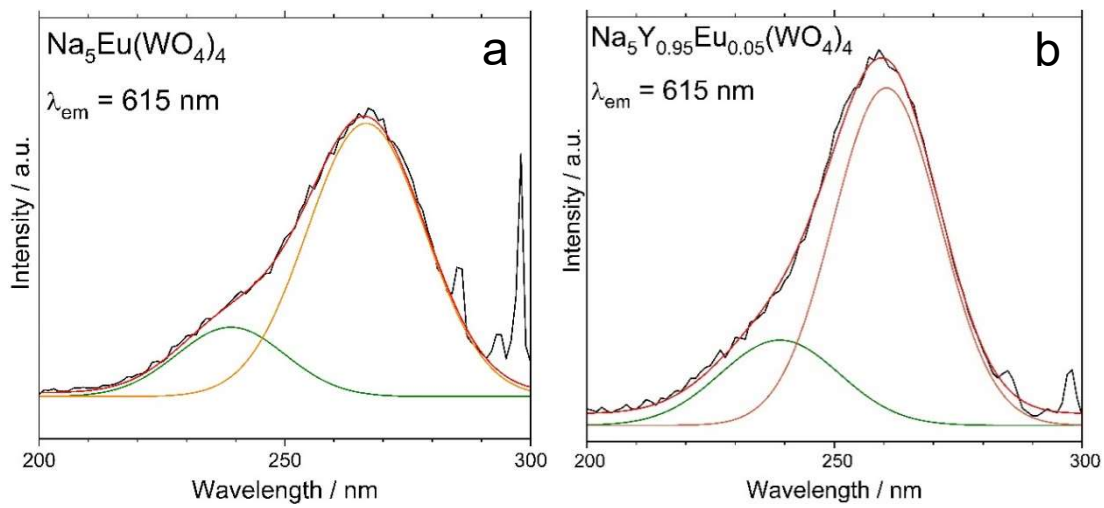


Fig. S21: Gaussian fit of the excitation spectra of $\text{Na}_5\text{Eu}(\text{WO}_4)_4$ (a) and $\text{Na}_5\text{Y}_{0.95}\text{Eu}_{0.05}(\text{WO}_4)_4$ (b): they were fitted using two peaks centred at 239 nm (O^2-W^{6+} LMCT) for both spectra and at 266.5 nm (a) and 260.5 nm (b) ($\text{O}^2-\text{Eu}^{3+}$ LMCT), respectively; the excitation spectra are corrected with respect to the lamp intensity.

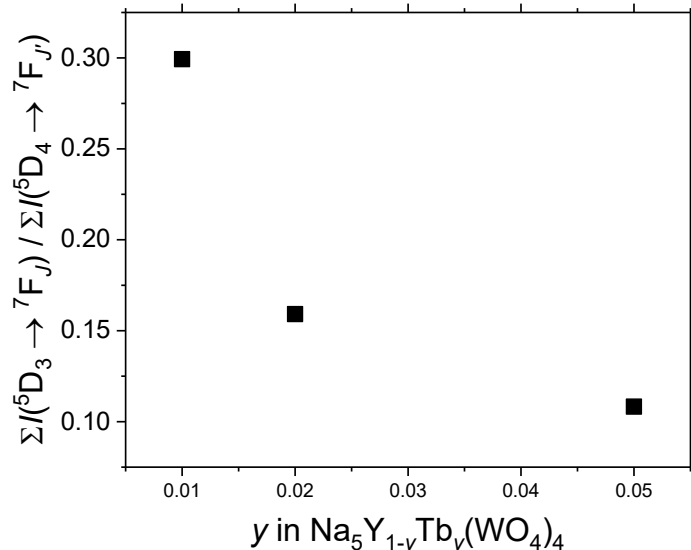


Fig. S22: Trend of the ratio of the emission intensity related to the ${}^5\text{D}_4 \rightarrow {}^7\text{F}_5$ transitions and the ${}^5\text{D}_4 \rightarrow {}^7\text{F}_5$ transition of Tb^{3+} varying with y in $\text{Na}_5\text{Y}_{1-y}\text{Tb}_y(\text{WO}_4)_4$.

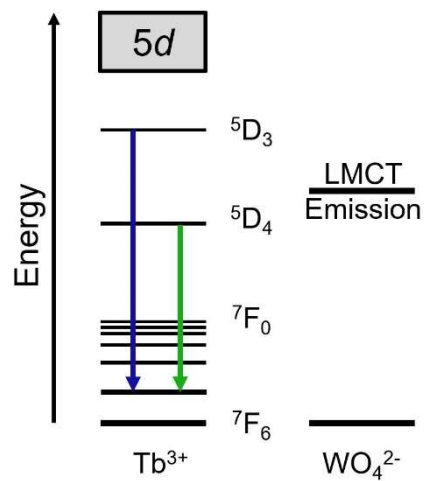


Fig. S23: Energy Levels of the Tb^{3+} f-states compared to the energy of the $\text{W}^{6+}\text{-O}^{2-}$ LMCT: The transferred energy is sufficient to reach the green emitting $^5\text{D}_4$ state, only. Consequently, no blue emission originating in the $^5\text{D}_3$ state is observed when exciting the WO_4^{2-} ion's LMCT.

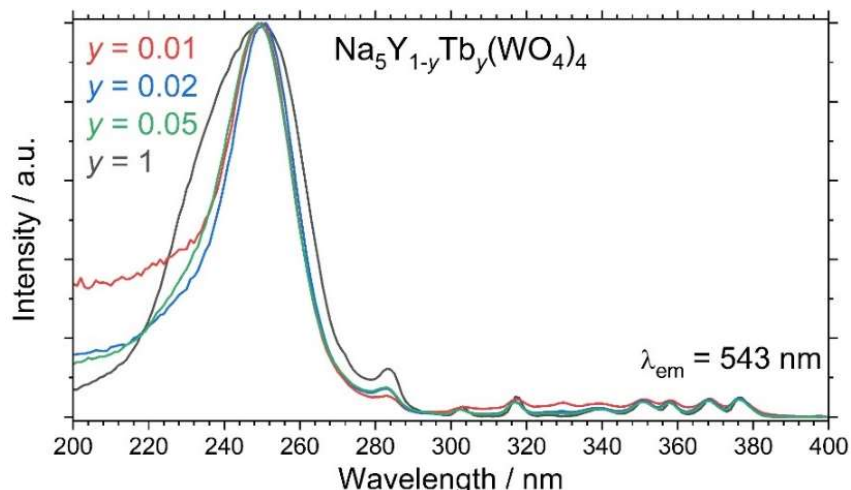


Fig. S24: Excitation spectra of $\text{Na}_5\text{Y}_{1-y}\text{Tb}_y(\text{WO}_4)_4$ ($y = 0.01, 0.02, 0.05, 1$) showing an increase of the intensity ratio of the broad LMCT band around 250 nm and the f-f transitions of Tb^{3+} with decreasing Tb^{3+} content.

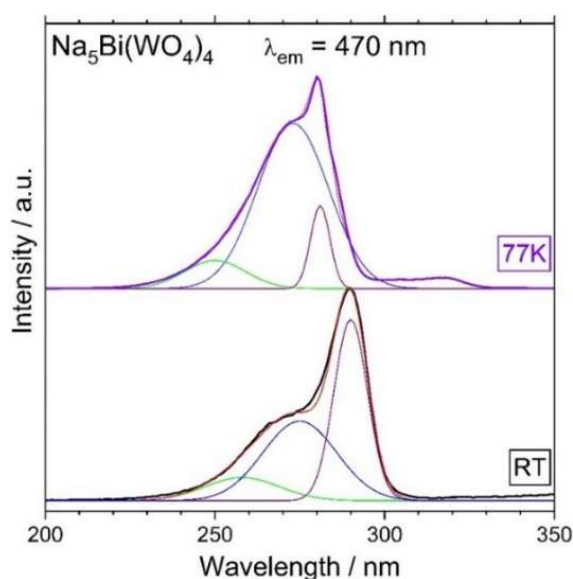


Fig. S25: Gaussian fit of the excitation spectra of $\text{Na}_5\text{Bi}(\text{WO}_4)_4$ at both room temperature and 77K. The excitation spectra are not corrected with respect to the lamp intensity.

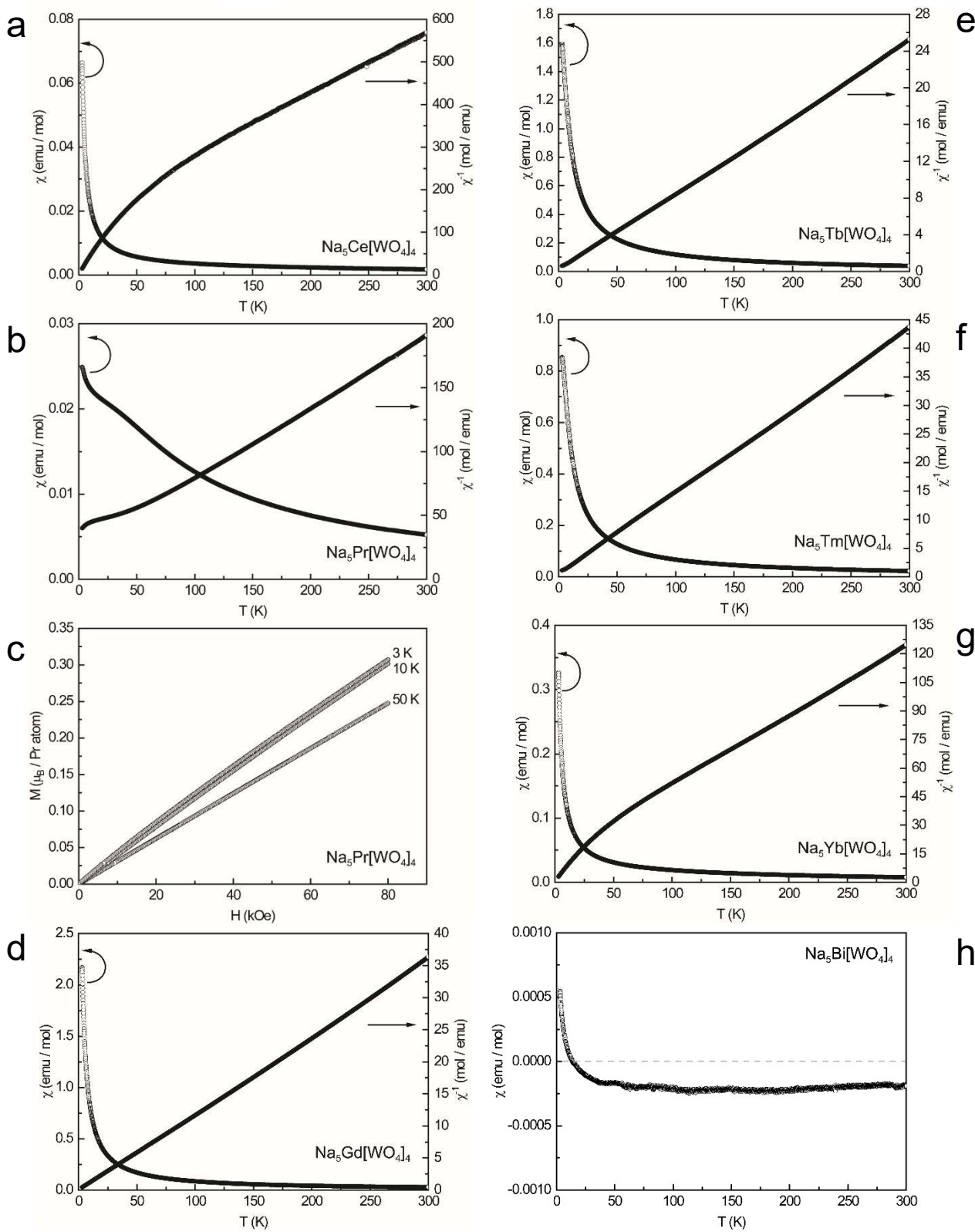


Fig. S26: Magnetic properties of $\text{Na}_5\text{M}(\text{WO}_4)_4$: temperature dependence of the magnetic susceptibility (χ and χ^{-1} data) measured at 10 kOe of magnetic properties of (a) $\text{Na}_5\text{Ce}(\text{WO}_4)_4$, (b) $\text{Na}_5\text{Pr}(\text{WO}_4)_4$, (d) $\text{Na}_5\text{Gd}(\text{WO}_4)_4$, (e) $\text{Na}_5\text{Tb}(\text{WO}_4)_4$, (f) $\text{Na}_5\text{Tm}(\text{WO}_4)_4$, (g) $\text{Na}_5\text{Yb}(\text{WO}_4)_4$ and (h) $\text{Na}_5\text{Bi}(\text{WO}_4)_4$; (c) magnetic properties of $\text{Na}_5\text{Pr}(\text{WO}_4)_4$: magnetisation isotherms at 3, 10 and 50 K.

References

- 1 R. D. Shannon, *Acta Cryst A*, 1976, **32**, 751–767.
- 2 T. Balić Žunić and E. Makovicky, *Acta Cryst Sect A Found Cryst*, 1996, **52**, 78–81.
- 3 E. Makovicky and T. Balić-Žunić, *Acta Crystallogr B Struct Sci*, 1998, **54**, 766–773.
- 4 H. Bärnighausen, *MATCH, Communications in Mathematical Chemistry*, 1980, **9**, 139–175.
- 5 U. Müller, *Z. Anorg. Allg. Chem.*, 2004, **630**, 1519–1537.
- 6 A. D. Fortes, *Acta Crystallogr., Sect. E: Crystallogr. Commun.*, 2015, **71**, 592–596.
- 7 C. W. F. T. Pistorius, *J. Chem. Phys.*, 1966, **44**, 4532–4537.
- 8 D. Huang, Y. Zhou, W. Xu, Z. Yang, M. Hong and J. Yu, *J. Lumin.*, 2012, **132**, 2788–2793.
- 9 D. Huang, Y. Zhou, W. Xu, Z. Yang, Z. Liu, M. Hong, Y. Lin and J. Yu, *J. Alloys Compd.*, 2013, **554**, 312–318.
- 10 D. Qin and W. Tang, *RSC Adv.*, 2016, **6**, 45376–45385.
- 11 J. Dong, X. Wang, L. Song, J. Yang, H. Wu, C. Yang and S. Gan, *Dalton Trans.*, 2018, **47**, 15061–15070.
- 12 S. Tanimizu, in *Phosphor handbook*, ed. H. Yamamoto, S. Shionoya and W. M. Yen, Taylor & Francis distributor, Boca Raton, Fla, London, 2nd edn., 2007, pp. 155–273.
- 13 W. T. Carnall, P. R. Fields and K. Rajnak, *J. Chem. Phys.*, 1968, **49**, 4424–4442.
- 14 W. T. Carnall, P. R. Fields and K. Rajnak, *J. Chem. Phys.*, 1968, **49**, 4450–4455.
- 15 W. T. Carnall, P. R. Fields and B. G. Wybourne, *J. Chem. Phys.*, 1965, **42**, 3797–3806.
- 16 J. Liao, S. Zhang, H. You, H.-R. Wen, J.-L. Chen and W. You, *Opt. Mater.*, 2011, **33**, 953–957.
- 17 M. Daub, A. J. Lehner and H. A. Höppe, *Dalton Trans.*, 2012, **41**, 12121–12128.
- 18 J.P.M. van Vliet and G. Blasse, *J. Solid State Chem.*, 1990, **85**, 56–64.
- 19 F. B. Xiong, Z. W. Zhang, H. F. Lin, L. J. Wang, Y. C. Xu and W. Z. Zhu, *Opt. Mater.*, 2015, **42**, 394–398.
- 20 N. Saito, N. Sonoyama and T. Sakata, *BCSJ*, 1996, **69**, 2191–2194.
- 21 S.-B. Kim, B. G. Kum, H. M. Jang, A. Lakshmanan and B. k. Kang, *J. Lumin.*, 2011, **131**, 1625–1628.
- 22 J. Liao, B. Qiu, H. Wen, J. Chen, W. You and L. Liu, *J. Alloys Compd.*, 2009, **487**, 758–762.
- 23 X. Shi, M. S. Molokeev, X. Wang, Z. Wang, Q. Zhu and J.-G. Li, *Inorg. Chem.*, 2018, **57**, 10791–10801.
- 24 Y. Liu, G. Liu, J. Wang, X. Dong and W. Yu, *Inorg. Chem.*, 2014, **53**, 11457–11466.
- 25 K. Binnemans, *Coord. Chem. Rev.*, 2015, **295**, 1–45.
- 26 G. Blasse, *J. Solid State Chem.*, 1972, **4**, 52–54.
- 27 P. Dorenbos, *J. Phys.: Condens. Matter*, 2003, **15**, 8417–8434.
- 28 H. E. Hoefdraad, *J. Solid State Chem.*, 1975, **15**, 175–177.